Earth-Science Reviews 197 (2019) 102915

Contents lists available at ScienceDirect

Earth-Science Reviews

journal homepage: www.elsevier.com/locate/earscirev

Climate as a factor for Neolithic cultural collapses approximately 4000 years BP in China

Qianli Sun[a], Yan Liu[a], Bernd Wünnemann[a,b,*], Yajun Peng[a], Xuezhong Jiang[c], Lanjie Deng[a], Jing Chen[a], Maotian Li[a], Zhongyuan Chen[a]

[a] State key laboratory of Estuarine and Coastal Research, East China Normal University, Shanghai 200062, China
[b] Institute of Geographical Sciences, Freie Universität Berlin, Malteserstr. 74-100, Berlin 12249, Germany
[c] School of Urban & Regional Science, East China Normal University, Shanghai, 200062, China

ARTICLE INFO

Keywords:
4000 yr BP
Climate change
Neolithic culture collapses
Asian Summer Monsoons

ABSTRACT

Although archaeological findings show the synchronous collapses of major well-documented Chinese Neolithic cultures around 4000 cal. yr BP, the driving mechanism for the phenomenon is still unclear and debatable. Spatial climatic features in China spanning this time period suggest a generally cold-dry setting. This is evidenced by 130 well-dated geological records at 97 sites located in climatically and topographically diverse regions, with occurrences of some extreme hydrological events like severe floods in the Chinese Loess Plateau, and in basins of the lower Yellow River and the middle-to-lower Yangtze River. The weakening of the Asian Summer Monsoon (ASM) since the mid-Holocene would have made Neolithic subsistence living unfavourable by decreasing the warmth and wetness in arid and semi-arid regions. However, it might not have been the sole factor that destroyed the Neolithic cultures in the vast territories of China *ca.* 4000 cal. yr BP. Environmental alterations in the major cultural territories of China reacted in response to precipitation anomalies caused by high variability of the ASM and the westerlies, which were modulated by centennial- to inter-annual- scale driving factors such as solar insolation, the North Atlantic Oscillation (NAO), the Pacific Decadal Oscillation (PDO) and El Niño-Southern Oscillations (ENSO). This most likely accounted for the nearly synchronous Chinese Neolithic cultural collapses.

1. Introduction

Exploring the link between rapid climate change and human adaptation during the Holocene, is an effort to better understand the mechanism-response patterns on global, regional and local scales. It is of broad interest to geo-archaeological communities (e.g. Weiss et al., 1993; Wu and Liu, 2004; Kuper and Kropelin, 2006; Turner and Sabloff, 2012; Clarke et al., 2016; Guo et al., 2018; Zheng et al., 2018). The rapid climate deterioration *ca.* 4.2 cal. kyr BP (deMenocal, 2001; Staubwasser et al., 2003), or at *ca.*4.2-3.8 cal. kyr BP (e.g. Mayewski et al., 2004), at *ca.* 4.8-4.5 cal. kyr BP (e.g. Wanner et al., 2011) or at *ca.* 2350-1850 cal. yr BC (e.g. Lillios et al., 2016) is more concerned as a significant event during the Holocene epoch (Anderson et al., 2007). It has been hypothesized that such a cold-dry climate period caused extensive human migration and collapse of cultures of many agriculture-based societies in areas across the northern Hemisphere such as the Nile valley, Mesopotamia, the Indus valley, and mid-continental North America (Cullen et al., 2000; Staubwasser et al., 2003; Booth et al., 2005; Kaniewski et al., 2018). In China, this event around 4000 years cal. yr BP (*ca.*4200-3800 cal. yr BP, with 200 years dating uncertainty) also exhibited a marked climate anomaly which altered the hydrological regime, resulting in a sharply contrasting environmental framework of drought in the north and flooding in southern China as described by some scholars (Wu and Liu, 2004; Tan et al., 2018). Major agriculture-based Neolithic cultures underwent nearly synchronous collapses in both semi-arid and monsoonal regions centring at/around 4000 cal. yr BP. Well-known in China are the collapses of the Qijia Culture in the Gansu-Qinghai region (An et al., 2005; Liu et al., 2010), the Laohushan and the lower Xiajiadian Culture (Shuangtouzi I period) in central-south Inner Mongolia (Tian and Akiyama, 2001; Tarasov et al., 2006), the Shijiahe Culture in the middle reaches of the Yangtze River (Wu and Wu, 1998; Yasuda et al., 2004), the Longshan Culture in the Shandong Peninsula, and the Liangzhu Culture in the lower Yangtze River basin (Chen et al., 2005; Zhang et al., 2005; Gao et al., 2007; Chen et al., 2011).

The dynamics and social effects of this event in China are spatially

* Corresponding authors.
E-mail addresses: qlsun@sklec.ecnu.edu.cn (Q. Sun), wuenne@zedat.fu-berlin.de (B. Wünnemann).

https://doi.org/10.1016/j.earscirev.2019.102915
Received 30 March 2019; Received in revised form 24 July 2019; Accepted 25 July 2019
Available online 26 July 2019

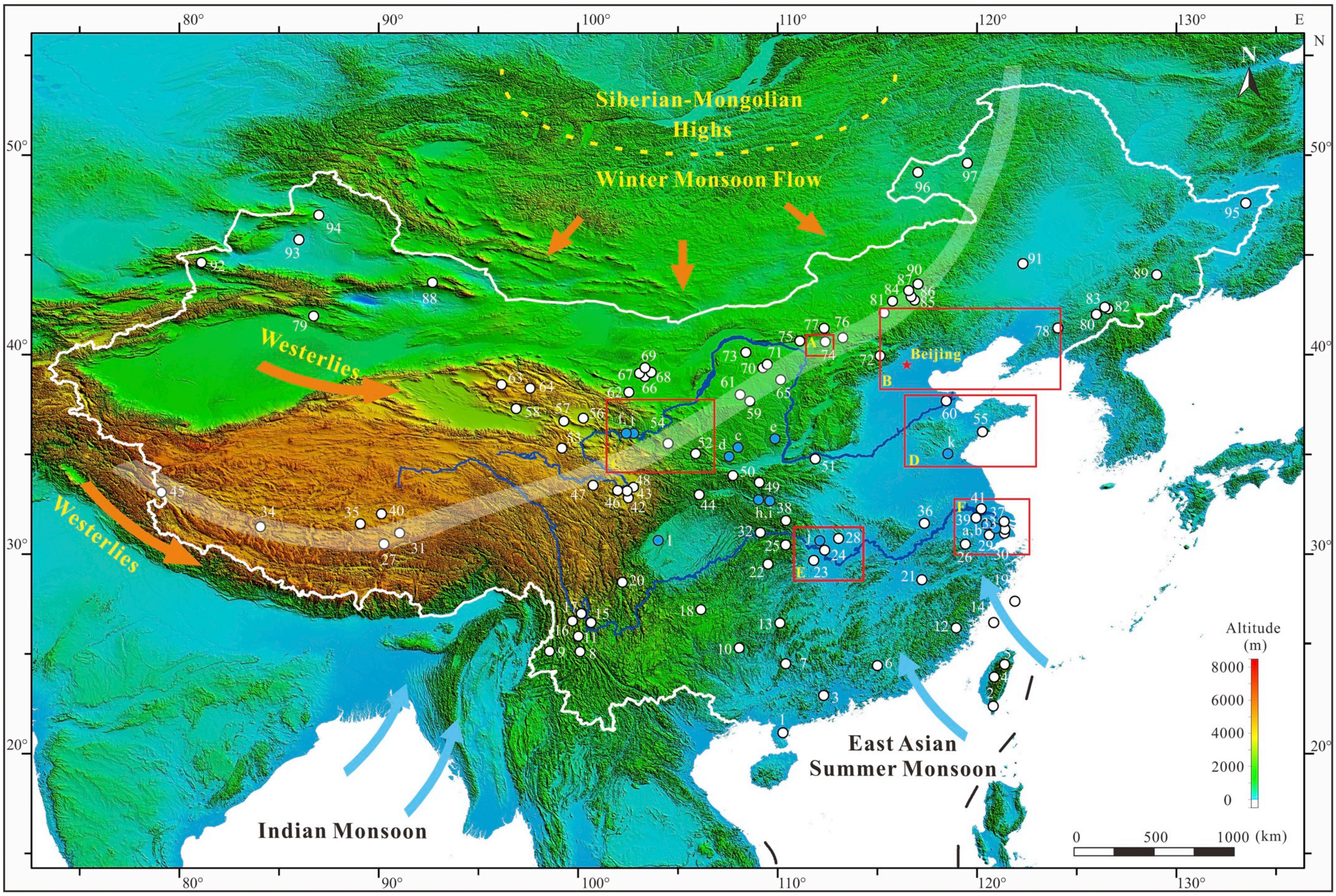

Fig. 1. Overview map with information of different climate zones and topographical conditions in China (modified after Xiao et al., 2004; Wünnemann et al., 2018; http://gdem.ersdac.jspacesystems.or.jp). Transitional zone (shadow belt) separates the arid region of north and northwest China and the monsoonal regions of east and south China. The locations of used records for climate change are marked in white dots and records for extreme/catastrophic floods are marked in blue dots (details in Tables 1-2). Six territories (A-F) of Neolithic cultures are also illustrated. A:the Daihai lake basin; B: north inner-Mongolia-Hebei and west Liaoning; C: the Dongting lake catchment; D the Gansu-Qinghai region; E: The Yangtze delta.

complex and rather ambiguous from local to regional scales. Various assumptions were proposed for the collapses of such highly complex societies during the Neolithic-Bronze cultural transition in different cultural territories, including abrupt climate changes, civil clan conflicts, catastrophic disasters, and an unsustainable treasury/populace (e.g. Wu and Wu, 1998; Zhao, 1999; Yu et al., 2000; Wu and Liu, 2004; Yuan, 2013; Wu et al., 2016). However, the almost synchronous cultural collapses may instead have resulted from some large-scale mechanism or a combination of multiple driving forces, and thus is worthy of further exploration.

The climate and diverse topography of China shows characteristic settings within different terrains. The eastern and southern part of China are topographically lowland regions and dominated by the influence of the Asian summer Monsoon (ASM), while the highland regions in the west and northwest are considered as arid to semi-arid climate, and are mainly influenced by the mid-latitude westerlies (MLW) (Fig. 1). The marginal zone between these two regions is considered to be a monsoonal-arid transition belt, which extends in a NE-SW direction along the boundary of the modern summer monsoon limit. This region is highly sensitive to the interactions of humid monsoonal and arid air-masses (Gao, 1962; Zhang and Lin, 1992). Given its various geographic features and plentiful records of prehistoric human occupation, China serves as an ideal place to study the mechanism-response pattern with a comprehensive perspective.

In this study, geological records with independent chronologies encompassing the period *ca.* 4000 cal. yr BP in China are collected (Fig. 1) to calculate the spatial differences within different atmospheric systems, including extreme hydrological events such as floods and droughts. Cultural collapses in various regions of China are then discussed from a geo-archaeological perspective. We aim to propose a mechanism-response of climate variations and cultural collapses around 4000 cal. yr BP in China which is interlinked with possible driving forces of different time scales.

2. Data sources and methods

2.1. Selection of climate records

In total, we collected 130 sequences of climate and environment reconstructions at 97 individual sites reported by researchers during recent decades with a wide spatial distribution covering different climatic and topographic regions of China (Fig. 1, Table 1). These included 16 sites in the arid regions of western China, 50 sites in the humid monsoonal domain region of eastern and southern China, and 31 sites in the semi-arid/arid regions along/west of the transitional belt and the Tibetan Plateau (Fig. 1, Table 1). The palaeoclimatic archives mainly consisted of lake cores, sediment sections (river, peat, desert, and archaeological), sediment trenches/outcrops, stalagmites, ice core, and other boreholes. Major requirements for each selected site comprised a well-established chronology as well as a consistent interpretation of proxy data with a sufficient resolution. These selected sites allowed us to estimate spatial differences of climate conditions in China

Table 1
Detailed information of the 130 climate records from 97 sites referred to in the text and figures with key references. See Fig. 1 for locations.

Record No.	Site No.	Site	Location			Archive	Dating No.s
			Lat.(N)	Long. (E)	Altitude (meters amsl)		
1	1	Huguangyan Maar	21.03°	110.28°	70	lake core	44^{*}
2						lake core	10^{*}
3	2	Dongyuan Basin	22.16°	120.83°	330-500	lake core	11^{*}
4	3	Hedong village	22.90°	112.33°	10	lacustrine section	8^{*}
5	4	Toushe	23.82°	120.88°	650	peat core	13^{*}
6	5	Retreat Lake	24.48°	121.43°	2230	lake core	10^{*}
7							
8	6	Dingnan	24.68°	115.00°	240	peat section	16^{*}
9			24.25°	115.03°		peat section	17^{*}
10			24.25°	115.03°		peat section	12^{*}
11	7	Panlong Cave	24.95°	110.36°		stalagmite	25^{*R}
12	8	Yuju Peak	25.10°	100.10°	3820	lacustrine section	4^{*}
13	9	Qinghai	25.12°	98.57°	1885	lake core	17^{*}
14	10	Dongge cave	25.28°	108.08°	680	stalagmite	$45^{\#}$
15							$45^{\#}$
16	11	Erhai	25.87°	100.02°	1961	lake core	7^{*}
17	12	Pingnan	26.05°	119.03°	1007	bore hole	7^{*}
18	13	Daping swamp	26.53°	110.13°	1620	swamp core	8^{*}
19	14	Core MZ01, ECS	26.55°	120.85°	-64.7	marine core	5^{*}
20							
21	15	Chenghai	26.56°	100.65°	1503	lake core	16^{*}
22	16	Tiancai Lake	26.63°	99.72°	na	lake core	18^{*}
23	17	Haligu	27.00°	100.17°	3277	lacustrine section	4^{*}
24	18	Dark cave	27.20°	106.17°	na	stalagmite	$28^{\#}$
25	19	MD06, ECS	27.73°	121.77°	-47	marine cores	11^{*}
26	20	Shayema	28.58°	102.22°	2453	lake core	5^{*R}
27	21	Shennong cave	28.70°	117.25°	383	stalagmite	$15^{\#}$
28	22	Lianhua Cave	29.48°	109.53°	455	stalagmite	$10^{\#}$
29							$42^{\#}$
30	23	Liyang plain	29.67°	111.82°	na	archaeological section	7^{*}
31	24	Jianghan plain	30.18°	112.37°	42.32	archaeological section	6^{*}
32	25	Heshang Cave	30.45°	110.42°	294	stalagmite	$21^{\#}$
33	26	Qianmutian	30.48°	119.43°	1338	peat section	4^{*}
34	27	Nam Co	30.50°	90.27°	4718-4722	lake core	12^{*}
35							27^{*}
36	28	Jianghan plain	30.77°	113.07°	33	outcrop	6^{*}
37	29	Pingwang	30.95°	120.63°	1.6	borehole	5^{*}
38	30	Maqiao site	31.03°	121.39°	4.5	archaeological section	6^{*}
39	31	Cuoe	31.05°	91.05°	4532	lake core	10^{*}
40	32	Dajiu Lake	31.07°	109.15°	1760	peat section	10^{*}
41							
42							
43	33	Core ZX-1,YD	31.25°	121.19°	na	borehole	7^{*R}
44			31.22°	121.63°			7^{*R}
45	34	Zabuye	31.35°	84.07°	4421	lake core	17^{*R}
46	35	Siling Co	31.5-32.0°	88.5°-89.5°	4530	lake core	17^{Δ}
47	36	Chaohu Lake	31.52°	117.37°	27	lake core	4^{*R}
48			31.55°	117.38°			6^{*}
49	37	Core CM97	31.62°	121.38°	2.48	borehole	10^{*}

(continued on next page)

Table 1 (*continued*)

Record No.	Site No.	Site	Location			Archive	Dating No.s
			Lat.(N)	Long. (E)	Altitude (meters amsl)		
50	38	Shanbao Cave	31.67°	110.43°	na	stalagmite	$14^{\#}$
51	39	Taihu Plain	31.30°	119. 09°	4-8	borehole	10^{*}
52	40	Zigentang Co	32.00°	90.15°	4560	lake core	5^{*}
53	41	Core HQ98	32.25°	120.23°	5.91	borehole	15^{*}
54	42	Hongyuan	32.77°	102.05°	3446	peat section	15^{*}
55			33.05°	102.05°	3446	peat section	16^{*}
56			33.77°	103.05°	3447	peat section	7^{*}
57	43	Zoige	33.45°	102.63°	3467	peat section	19^{*}
58	44	Xianglong cave	33.00°	106.33°	940	stalagmite	$58^{\#}$
59	45	Bangong Co	33.07°	79.00°	4241	lake core	25^{*R}
60	46	Zoige basin	33.10°	102.66°	3470	peat section	20^{*}
61	47	Ximencuo	33.38°	101.10°	4030	lake core	13^{*}
62							
63	48	Tangke	33.45°	102.63°	3454	peat section*	7^{*}
64	49	Jiuxian Cave	33.57°	109.10°	1495	stalagmite	$23^{\#}$
65	50	Sanqing Chi	33.93°	107.77°	3080	lacustrine section	6^{*}
66	51	Mengjin	34.80°	112.41°	na	lacustrine section	4^{*}
67	52	Dadiwan	35.02°	105.90°	1400	river section	4^{*R}
68	53	Kuhai Lake	35.30°	99.20°	4132	lake cores	32^{*}
69							$60^{*}25^{\Delta}$
70	54	Sujiawan	35.53°	104.52°	1700	river section	3^{*}
71	55	Qingdao	35.58°-37.15°	119.50°-121°	na	sediment core	5^{*}
72	56		36.62°-37.08°	100.42°-100.92°	3300	outcrop	$8^{*}/12^{\Delta}$
73			36.53°	99.36°	3200	lake core	10^{*}
74		Qinghai Lake					
75			36.80°	100.13°	3194		65^{*}
76	57	Chaka salt Lake	36.63°	99.03°	3200	lake core	10^{*}
77	58	Hurleg Lake	37.28°	96.90°	2817	lake core	19^{*}
78	59	Midiwan	37.65°	108.62°	1400	peat section	21^{*R}
79	60	Yellow River delta	37.67°	118.47°	5.5	sediment core	23^{*}
80	61	Jingbian	37.98°	108.13°	na	outcrop	11^{*}
81	62	Hongshui River	38.17°	102.75°	1460	river section	9^{*}
82	63	Dunde	38.17°	96.40°	5325	ice core	
83	64	Halal lake	38.30°	97.60°	4078	lake core	31^{*}
84							10^{*}
85	65	Jinjie, MUD	38.73°	110.17°	1159	peat section	$1^{*}10^{\Delta}$
86							
87	66	Zhuyeze	39.02°	103.33°	1320	lacustrine section	$12^{*}12^{\Delta}$
88	67	Qingtu Lake	39.05°	103.07°	1309	lacustrine section	$20^{*}6^{\Delta}$
89	68	Minqin Basin	39.05°	103.08°	na	lacustrine section	9^{*}
90	69	Yiema Lake	39.10°	103.67°	na	lacustrine section	7^{*R}
91	70	Baahar Nuur	39.32°	109.27°	1278	lake core	16^{*R}
92							15^{*R}
93	71	Qigai Nuur	39.5°	109.5°	na	lake core	17^{*}
94	72	Taishizhuang	40.07°	115.08°	150	peat section	6^{*}
95	73	Yanhaizi	40.10°	108.42°	1180	lake core	17^{*}
96	74	Daihai	40.58°	112.07°	1200	lake core	8^{*}
97							8^{*}
98							11^{*}
99	75	Chasuqi	40.67°	111.13°	1000	peat section	4^{*R}
100	76	Huangqihai	40.83°	113.28°	1308	lake core	15^{*}
101	77	Diaojiao lake	41.30°	112.35°	1800	lake core	4^{*R}
102	78	Water cave	41.32°	124.07°	na	stalagmite	na

(*continued on next page*)

Table 1 (*continued*)

Record No.	Site No.	Site	Location			Archive	Dating No.s
			Lat.(N)	Long. (E)	Altitude (meters amsl)		
103	79	Bosten lake	41.94°	86.76°	1049	lake core	5*
104			41.90°	86.72°	1049	lake core	5*
105	80	Gushantun	42.00°	126.00°	500	marsh section	10*
106	81	Bayanchagan	42.08°	115.35°	1355	trench section	9*
107	82	Sihailongwan	42.28°	126.60°	797	lake core	36*
108							40*
109	83	Jinchuan	42.37°	126.43°	662	peat section	6*
110	84	Lake Xiarinur	42.61°	115.45°	na	lake core	17*
111	85	Otindag	42.66°	115.95°	na	lacustrine section	11$^{\Delta}$
112	86	Haolaihure lake	42.95°	116.62°	1295	lacustrine section	12*
113	87	Dali Lake	43.25°	116.48°	1220	outcrops	36*9$^{\Delta}$
114			43.27°	116.61°		lake core	12*
115	88	Balikun Lake	43.60°	92.77°	1575	lake core	13*
116				92.70°	1575		12*
117					1580	lacustrine section	7*
118	89	Jingpo lake	43.98°	129.03°	350	lake core	13*
119	90	Hunshandake sandy	42.50°-43.50°	116.40°-117.50°	na	outcrop	23$^{\Delta}$
120		lands					16$^{\Delta}$
121	91	Liuhutun	44.46°°	123.13°	151	outcrop	7*
122	92	Sayram Lake	44.58°	81.15°	2072	lake core	12*
123	93	Manasi Lake	45.75°	86.00°	251	lake core	9*R
124							
125	94	Wulungu Lake	46.98°	87.00°	478.6	lake core	7*
126	95	Sanjiang Plain	47.58°	133.50°	71	peat core	8*
127	96	Hulun lake	49.12°	117.05°	545.3	lake core	12*
128							13*
129							6*
130	97	Hulunbeier	49.58°	119.53°	na	desert section	20$^{\Delta}$

Record No.	Sequence range (kyr/ka)	Event range (kyr/ka)	Description *c*.4.0 kyr/ka BP	Coding (this study)		Major prox (ies)	References
				Warmth	Humidity		
1	50-0	4.25-3.85	cool/dry	2	2	dry density	Liu et al., 2000
2	11.6-0	~4.2	cool/dry			pollen	Wang et al., 2007
3	17-0	4.1-2.1	cool	2		pollen	Lee and Liew, 2010
4	4.5-0	4.0-3.3	cold/dry	1	2	GS, humification, TOC	Zhong et al., 2014
5	11.2- 0	~4.0	cold	1		pollen	Liew et al., 2006
6	10.3-0	4.5-2.1	dry	1	2	OM, MS, EL	Selvaraj et al., 2007
7		4.5-2.1	cold/dry			pollen, EL, n-alkane	Wang et al., 2014
8	18.3-0	4.4-4.25	cold/dry	1	2	OM. $\delta^{13}C_{org}$, CAR	Wei et al., 2018
9	18.0-0	4.0-3.8	dry			pollen, OM, GS	Zhou et al., 2004
10	15.6-0	4.0-3.8	dry			TOC, pollen, n-alkane	Zhou et al., 2005
11	11.3- 0	4.4-2.6	cold/dry	1	2	$\delta^{18}O$	Li et al., 1998
12	10.3-0	~4.0	dry		2	GS, MS, pollen, geochemistry	Yang et al., 2010
13	18.3-0	~4.0	dry		2	GS, Titanium	Zhang et al., 2017
14	16.0-0	~3.5	dry		2	$\delta^{18}O$	Dykoski et al., 2005
15	9.0-0	4.5-4.0	dry			$\delta^{18}O$	Wang et al., 2005
16	12.0-0	4.4-3.9	cold/dry	1	2	MS, Pollen	Dearing et al., 2008
17	40.0-0	4.4-2.6	cool	2		pollen	Yue et al., 2012
18	14.6-0	4.0-3.5	cool/dry	2	2	GS, pollen	Zhong et al., 2015

(*continued on next page*)

Table 1 (*continued*)

Record No.	Sequence range (kyr/ka)	Event range (kyr/ka)	Description *c*.4.0 kyr/ka BP	Coding (this study)		Major prox (ies)	References
				Warmth	Humidity		
19	8.0-0	4.2-2.3	cold/dry	1	2	GS, EL, magnetism	Liu et al., 2013
20		~4.2	cool			EL, foraminifera	Li et al., 2015
21	8.3-0	4.67-3.47	decline warmth / wet	2	2	pollen, charcoal	Xiao et al., 2018a
22	11.7-0	3.9-3.8	dry		2	pollen	Xiao et al., 2014
23	9.0-0	4.0-2.4	moderate/wet	3	3	pollen	Song et al., 2012
24	6.1-0	4.4-4.1	dry		2	$\delta^{18}O$	Jiang et al., 2013a
25	10-0	4.4-3.8	cold	1		TOC/TN, $U_{37}^{K'}$	Kajita et al., 2018
26	11.0-0	~4.4	cool/dry	2	2	Pollen	Jarvis, 1993
27	5.3-3.6	4.2-3.9	wet		3	$\delta^{18}O$, $\delta^{13}C$	Zhang et al., 2018
28	6.5- 0	~4.0	dry		2	$\delta^{18}O$	Cosford et al., 2008
29	12.5-0	~4.2	dry			$\delta^{18}O$	Zhang et al., 2013
30	5.0-2.5	4.2-4.0	cool/dry	2	2	pollen, geochemistry	Guo et al., 2016
31	12.7-0	4.4-4.1	dry		2	GS, EL	Li et al., 2014
32	9.45-0	4.8-4.1	dry		2	$\delta^{18}O$	Hu et al., 2008
33	5.0-0	~4.2	dry		2	humification	Ma et al., 2009
34	8.4-0	6.9-2.9	cold/dry	1	2	GS, TOC, TN, n-alkanes, minerals	Zhu et al., 2008b
35	8.3-0	4.0-3.7	dry			GS, OM, EL, $\delta^{13}C$ (n-alkanes)	Mügler et al., 2010
36	4.6-4.0	4.2-4.0	dry		2	TOC, pollen, $\delta^{13}C_{org}$	Li et al., 2013
37	7.7-0	~4.2	cool	2		pollen	Innes et al., 2014
38	7.2-0	4.4-3.3	warm/dry	4	2	foraminifera, ostracods, pollen	Yu et al., 2000
39	10.5-1.6	4.6-4.0	cold/dry	1	2	Sr, TOC, C/N, $\delta^{13}C_{org}$	Wu et al., 2006
40	15.7-0	~4.2	cool/dry	2	2	TOC, C/N, $\delta^{13}C_{org}$	Ma et al., 2008
41		4.2-3.8	wet			aerobic hopanoids	Xie et al., 2013
42		~4.0	dry			pollen	Zhu et al., 2008a, 2010
43	13.0-0	~4.1	cold/dry	2	2	MS, Pollen	Tao et al., 2006
44	8.0- 0	~4.1	cool/wet			pollen	Chen et al., 2005
45	30.0-0	6.3-4.1	cold/dry	1	2	TOC, carbonates, $\delta^{13}C_{carb}$, $\delta^{18}O_{carb}$	Wang et al., 2002
46	15.0-0	4.0-3.6	dry		2	lake level	Shi et al., 2017
47	5.6-0	5.2-3.9	cold	2	2	phytolith	Fan et al., 2006
48	9.87-0	4.8-2.1	warm/dry			GS, pollen	Wang et al., 2008
49	11-0	4.8-3.8	cold/dry	1	2	pollen	Yi et al., 2006
50	11.5-2	4.3-4.0	dry		2	$\delta^{18}O$	Shao et al., 2006
51	13.0-0	4.4-4.0	cool/dry	2	2	pollen	Yao et al., 2017
52	11.5-0	4.1-3.5	cold/dry	1	2	pollen	Herzschuh et al., 2006
53	11.5-0	4.8-3.8	cold/dry	1	2	pollen	Yi et al., 2006
54	12.0- 0	~4.2	cold/drier	1	2	plant cellulose, $\delta^{13}C_{cel}$	Hong et al., 2003
55	9.6-0.3	4.2-3.7	cold/dry			carbon density, $\delta^{13}C_{org}$	Large et al., 2009
56	6.0-0	4.5-4.0	cold			$\delta^{18}O_{cel}$	Xu et al., 2002
57	10.0-0	4.6-3.3	cool/dry	2	2	micro-charcoal	Zhao et al., 2017
58	6.65-0	4.4-3.8	wet		3	$\delta^{18}O$, $\delta^{13}C$	Tan et al., 2018
59	10.0-0	4.3-3.4	dry		2	minerals, carbonate, $\delta^{18}O_{carb}$	Gasse et al., 1996
60	10.5-0	4.0-3.6	cold/dry	1	2	pollen, OM, carbonate	Sun et al., 2017b
61	13-0	4.7-3.7	cold/dry	1	2	GS, OM, EL, MS	Zhang and Mischke, 2009
62		4.2-2.8	cold			GS, TOC, $\delta^{13}C_{org}$, minerals	Mischke and Zhang, 2010
63	7.9-0	4.13-4.01	cool/dry	2	2	pollen	Guo et al., 2013
64	11.2-0	4.5-2.5	dry		2	$\delta^{18}O$	Cai et al., 2010
65	5.9-0	5.1-4.0	cold/dry	1	2	GS, magnetism, TOC, TN, pollen	Wang et al., 2016
66	6.9-3.2	4.04-3.83	cool/dry	2	2	EL	Dong et al., 2009
67	7.5-3.8	~4.0	drier		1	GS, TOC, carbonates, pollen	An et al., 2003
68	14-0	4.5-3.0	cold/dry	1	2	$\delta^{18}O_{bulk}$, carbonate, ostracod	Wünnemann et al., 2018
69		4.5-3.0				GS, ostracod, lake level	Yan et al., 2018
70	8.5-3.8	4.1-3.6	drier		2	GS, TOC, carbonate, pollen	An et al., 2003, 2005
71	7.25-0	4.55-3.90	cool	2		pollen	Chen and Wang, 2012

(*continued on next page*)

Table 1 (*continued*)

Record No.	Sequence range (kyr/ka)	Event range (kyr/ka)	Description *c*.4.0 kyr/ka BP	Coding (this study)		Major prox (ies)	References
				Warmth	Humidity		
72	12.5-0	4.0-2.6	cold/dry			GS, TOC, magnetism	Lu et al., 2015
73	18.0-0	4.2-2.3	dry			brightness, redness	Ji et al., 2005
74		4.5-2.5	cold/drier	1	2	pollen, carbonate, OM, $\delta^{13}C_{org}$	Shen et al., 2005
75	32-0	5.0-3.5	cold			$U_{37}^{K'}$	Hou et al., 2015
76	10.4-0	5.0~	dry		2	minerals, TOC, TN, carbonates	Liu et al., 2008
77	7.5-0	4.4-3.8	dry		2	magnetism, $\delta^{18}O_{carb}$, ostracod, EL	Zhao et al., 2010
78	13.0-0	~3.8	cold/dry	1	2	OM, pollen, $\delta^{13}C_{org}$	Li et al., 2003
79	12.0-0	4.5-2.7	cool/dry	2	2	pollen	Yi et al., 2003
80	10.0-0	5.5-2.7	warm/wet	4	3	GS, TOC	Xiao et al., 2002
81	8.5-3.0	4.3-3.7	cold/wet	1	3	EL, TOC, pollen, $\delta^{18}O_{carb}$, $\delta^{13}C_{carb}$	Zhang et al., 2000
82	4.5-0	4.5-3.9	cold	1		$\delta^{18}O$	Yao and Thompson, 1992
83	23.5-0	~4.1	cool/drier	1	1	OM, Ti, ostracod, $\delta^{18}O_{bulk}$	Yan and Wünnemann, 2014
84	23.5-0	5.0-3.0	cold			GS	Wang et al., 2015
85	7.0-0	4.1-3.7	relatively humid		3	GS, OM, EL	Liu et al., 2014
86		4.1-3.7				EL	Liu et al., 2015a
87	11.6-0	4.8-2.1	dry		2	GS, TOC, ostracod, lake level	Mischke et al., 2016
88	10.0-0	4.8-2.5	dry		2	GS, TOC, C/N, $\delta^{13}C_{org}$	Long et al., 2010
89	9.87-0	4.5-3.4	wet		3	MS, TOC, carbonates, pollen	Chen et al., 2001
90	11.3-1.3	4.7-3.2	dry		2	MS, GS, geochemistry	Chen et al., 1999
91	7.65-0	~4.2	cool	2	2	GS, MS, carbonates	Feng et al., 2005
92	17.0-0	~4.2	dry			pollen, TOC, $\delta^{13}C_{org}$, carbonate	Guo et al., 2007
93	9.0-0	4.0-2.8	cold/dry	1	2	GS, OM, pollen	Sun and Feng, 2013
94	6.2-0	4.4-3.6	dry		2	pollen/biome	Tarasov et al., 2006
95	14.0-0	4.3-3.2	cold/wet	1	3	MS, OM	Chen et al., 2003
96	10.0-0	4.4-3.1	dry			GS	Peng et al., 2005
97	10.0-0	4.4-3.9	cold/dry	1	2	pollen	Xiao et al., 2004
98	4.5-0	4.1-3.8	cold/dry			TOC, carbonates, geochemistry	Xu et al., 2017
99	9.1-0	4.4-2.5	moderate/dry	3	2	pollen	Wang and Sun, 1997
100	9.0-0	~4.0	cold/dry	1	2	pollen	Hao et al., 2014
101	10.0-0	4.9-3.2	moderate/dry	3	2	pollen	Shi and Song, 2003
102	6.0-0	4.0-3.0	dry		2	$\delta^{18}O$	Tan and Cai, 2005
103	8.6-0	4.0-2.0	dry		2	pollen, ostracods	Tarasov et al., 2019
104	8.5-0	~4.2	dry			Ostracods, EL	Mischke and Wünnemann, 2006
105	13.0-0	~4.2	cool/dry	2	2	GS, pollen	Li et al., 2017
106	12.5- 0	5.8-4.0	dry		2	pollen, carbonates, $\delta^{18}O_{carb}$	Jiang and Liu, 2007
107	15.0-0	4.1-3.6	dry	2	2	TOC, TN, biogenic silica	Schettler et al., 2006
108		4.0-2.9	cooling/dry			pollen	Stebich et al., 2015
109	5.5-0	4.2-2.0	cold/dry	1	2	pollen, charcoal	Jiang et al., 2008
110	15.6-0	~4.2	dry		2	GS, pollen, magnetism,	Tang et al., 2015
111	10.0-0	4.3-3.0	dry		2	MS, GS, TOC	Gong et al., 2013
112	12-0.3	4.6-3.7	warm/dry	4	2	GS, TOC, TN, $\delta^{13}C_{org}$	Liu et al., 2018
113	16.0-0	5.0-4.2	dry		2	Lake level	Goldsmith et al., 2017
114	12.8-0	4.45-3.75	dry			TOC, TN, lake level	Xiao et al., 2008
115	16.7-0	4.3-3.8	drier	1	2	pollen	Tao et al., 2010
116	8.5-0	4.3-3.8	cold/dry			GS, pollen, magnetism	An et al., 2012
117	9.3-0	4.0-2.0	cold/wet			EL	Zhong et al., 2012
118	6.4-0	5.1-3.6	warm/wet	4	3	pollen, $\delta^{13}C_{org}$	Chen et al., 2015
119	6.3-0	4.2-2.8	dry		1	lithology, diatom	Yang et al., 2015
120	11.0-0	4.2-3.8	drier			GS, OM	Scuderi et al., 2019
121	11.37-0	4.3-3.8	wet	1	2	MS, OM, carbonate	Zhao et al., 2018
122	17.9-0	5.5-3.4	cold/wet	1	3	pollen	Jiang et al., 2013b
123	11.8-0	4.2-3.7	dry		2	carbonates, pollen, diatoms	Rhodes et al., 1996
124		4.2-3.7				carbonate, pollen	Lin et al., 1996

(*continued on next page*)

Table 1 (*continued*)

Record No.	Sequence range (kyr/ka)	Event range (kyr/ka)	Description c.4.0 kyr/ka BP	Coding (this study)		Major prox (ies)	References
				Warmth	Humidity		
125	9.5-0	5.-3.6	moderate/wet	3	3	GS, pollen, $\delta^{13}C_{org}$, TOC, TN	Jiang et al., 2007
126	6.1-0	~4.0	dry		2	charcoal	Zhang et al., 2015b
127	9.6-0	4.3-3.35	cold/drier	1	1	ostracods, isotope, EL	Zhai et al., 2011
128	11.0-0	4.4-3.35	cold/drier			pollen	Wen et al., 2010
129	5.0-3.0	4.21-3.84	drier			GS, pollen, ostracods	Xiao et al., 2018b
130	11.0-0	4.4-1.8	dry		2	lithology	Li and Sun, 2006

ECS: East China Sea; MUD: Mu Us desert; YD: Yangtze delta

* Radiocarbon dating; $^{\Delta}$ Optically stimulated luminescence dating (OSL); $^{\#}$ Th^{230} dating; ^{R} radiocarbon age recalibrated.

GS: grain size; TOC: Total organic carbon; OM: organic matter; MS: magnetic susceptibility; EL: elements; CAR: carbon accumulation rate; $\delta^{13}C_{org}$: isotope of organic matter; $\delta^{13}C_{carb}$, $\delta^{18}O_{carb}$: isotope of carbonates; $\delta^{13}C_{cel}$, $\delta^{18}O_{cel}$: carbon and oxygen isotope of cellulose; $\delta^{18}O_{bulk}$: oxygen isotope of bulk sample.

with statistical significance on a regional scale.

2.2. Dates and chronology

The selected sequences of climate and environment reconstructions were based on well-established chronologies which mainly consisted of radiocarbon dates (n = 1372), optically stimulated luminescence dates (OSL) (n = 151) and Th^{230} dates (n = 301) from different records. To unify to the same unit, calendar ages were adopted for these records. Thus, fifteen records which used ^{14}C ages (n = 170) in some previous publications were recalibrated (mark with ^{R}) using the Calib 7.02 program with IntCal13 datasets in this study to meet the standard (Reimer et al., 2013) (Table 1). These re-calibrations refer to 2 sigma mean values.

2.3. Implications of proxies

Indicators of moisture and thermal changes for the above records included proxies such as geophysical data (e.g., lithology, grain-size and magnetic susceptibility), geochemical data (e.g. organic matter, carbonates, mineral and elemental composition, aerobic hopanoids, n-alkane, $U_{37}^{K'}$, stable carbon and oxygen isotopes), and biological data (e.g. pollen, diatoms and ostracods)(Table 1). Grain-size composition changes were interpreted in terms of different hydrological or aeolian regimes in relation to moisture changes, although the detailed climatic explanations were complex for different records and from site to site. For instance, the grain-size distribution of lake sediments reflects the dynamics of sediment transport and deposition depending on lake-catchment characteristics, representatives are the closed Daihai Lake in the monsoonal margin of north China and the closed Kuhai Lake in the northeast of Tibetan Plateau (TP) (e.g. Peng et al., 2005; Yan et al., 2018). However, increased aeolian activity due to a drier climate could also increase coarse grain size fraction in lake sediment in the arid regions, such as lakes in the lower Hei River catchment (e.g. Chen et al., 1999; Chen et al., 2003) (Table 1). For the aeolian deposits (e.g. loess/paleosol sequences, sand dunes) in monsoonal and arid transitional regions of north China, grain size frequently serves as a proxy index for the strength of monsoon winds at certain sites, strong winter monsoon winds from cold-dry climate usually bring coarser components in grain size (Xiao et al., 2002; An et al., 2003) (Table 1). Numerical unmixing of grain size distribution data into constituent components, known as end-member analysis (EMMA) can also act as a useful tool, unravelling the past environmental processes that help identifying climatic conditions under which the sediments were produced, transported and deposited. Examples were in the Hala Lake and Kuhai Lake (e.g. Wang et al., 2015; Yan et al., 2018).

Magnetism as a tool to reconstruct past environmental conditions is to identify changes in concentration, mineralogy and grain size of the mineral magnetic assemblage. Magnetic susceptibility (MS) of Lake Erhai sediment was used as a general proxy for silts/fine sands containing primary magnetite eroded from lake drainage under different hydrothermal settings (Dearing et al., 2008). Magnetic susceptibility also suggests the pedogenic processes controlled by precipitation, thus can serve as a proxy for the moisture changes of the aeolian deposits (e.g. Chen et al., 1999, 2011; Lu et al., 2015).

Geochemical approaches are useful to explore the mechanisms and causes of major changes in the environmental and climatic conditions of the earth. The organic matter (OM, TOC, TN) in the sediments is commonly seen as a direct reflection of the amount of organic inputs, the paleo-productivity and preservation conditions after deposition. In lake and bog systems, two principal sources, i.e., autochthonous, aquatic plants living in the lake water, and allochthonous, terrestrial plants growing in the lake catchment would reflect the aquatic biology, and vegetation and productivity of the lake catchment respectively. With C/N ratios, it can serve as an indirect indicator of the type and biomass of local vegetation, and thereby can potentially reflect changes in the regional precipitation. High total organic matter (TOC) and C/N ratio values normally reflect the increased precipitation during relatively humid and warm conditions. Conversely, their decreases were ascribed to a dry and cool or cold climate (e.g. Selvaraj et al., 2007; Zhong et al., 2014; Xu et al., 2017). While, for some peat sections in monsoonal regions of south China, low TOC with sand grains suggested wetter conditions with stream deposition, and high TOC suggests drier marshy (peat-forming) conditions (Zhou et al., 2004). For the aeolian deposits in north and northwest China, lower TOC values with coarser particle size of the sediment indicated strong aeolian activity from dry climate, and their highs suggested a relatively humid setting (e.g. Xiao et al., 2002; Long et al., 2010). Carbonates (aragonite, calcite and dolomite) in the lake sediment is a reflector of changes in carbonate equilibrium as a result of physical changes in the lake (e.g. evaporative loss from temperature), and/or of biological productivity when increased photosynthesis by submerged aquatic plants and algae removes dissolved CO_2. Generally, carbonates in lake sediment indicate the effective moisture changes by warmth and wetness of the lake drainage (e.g. Chen et al., 2003; Shen et al., 2005). Mineral and elemental composition of sediment is closely linked to the changes in sediment source, chemical weathering and hydrodynamic processes. Generally, more weathered elements are produced during warm and humid climate periods than during cold and dry regimes. The chemical composition of lake sediments can infer the chemical weathering and hydrothermal settings of the lake basin associated with climate changes such as in Daihai Lake basin (e.g. Xu et al., 2017). Titanium (Ti) is a conservative element that mainly comes from land-derived materials. It has been widely used as a proxy for catchment runoff and allochthonous sediment supply to the lake (e.g. Zhang et al., 2017; Wünnemann et al., 2018).

For the stable isotope signals, values of $\delta^{13}C_{org}$ from terrestrial organic matter can serve as a proxy for the vegetation changes between C_3 and C_4 plants. As C_3 plants are more sensitive to moisture changes, and more positive $\delta^{13}C_{org}$ values can be interpreted as at least partial evidence of aridity (e.g. Ma et al., 2008; Li et al., 2013; Liu et al., 2018). $\delta^{13}C_{cel}$ of C_3 plants (isotope of cellulose) in the peat deposits also indicate that the smaller the $\delta^{13}C$ of peat plant remains cellulose, the stronger the monsoon activity, and vice versa in the eastern margin of the TP (e.g. Hong et al., 2003). The $\delta^{18}O_{carb}$ in authigenic lake carbonate is a proxy of continental climate and depends on the isotopic composition of lake water and water temperature (e.g. Zhang et al., 2000; Zhao et al., 2010). Variations of $\delta^{18}O_{bulk}$ values in authigenic carbonate dominated lake sediments also act as a measure for positive or negative water balance and indirectly indicating changes in water depth or by hydro-climatic processes such as the impact of warm season of summer monsoon (e.g.Yan and Wünnemann, 2014; Wünnemann et al., 2018). Since the n-alkanes have strong resistance to alternation and degradation, they act as relatively durable paleoenvironmental proxies. The chain length of odd-carbon number n-alkanes are produced by higher vegetation ($> C_{25}$) and can be attributed to herbs (C_{31}, C_{33}) and trees (C_{27}, C_{29}). The distribution pattern and ratios between different chain length carbons may therefore indicate the sources of biomass and predominant vegetation type which is related to climate changes (e.g. Zhou et al., 2005; Wang et al., 2014). The aerobic hopanoids concentrations is closely associated with the changes of water-table depth of the peat deposits in Dajiuhu, central China, lower water tables will be characterized by higher hopanoid concentrations in the drier, more aerobic, surface zone than in the higher water levels (Xie et al., 2013).

Alkenone palaeothermometry ($U_{37}^{K'}$) is applied to quantify past temperature variation of the lake water and the sea water (e.g. Hou et al., 2015; Kajita et al., 2018). High-resolution speleothem $\delta^{18}O$ records were generally used to demonstrate local-moisture variations in relation to changes in vapour sources or the intensity of monsoon precipitation. (e.g., Tan and Cai, 2005; Wang et al., 2005; Hu et al., 2008; Tan et al., 2018).

Pollen assemblages were employed to infer vegetation changes in response to hydrothermal alternations, and statistically extracted quantitative precipitation estimates were used to reflect moisture changes (e.g. Xiao et al., 2004; Herzschuh et al., 2006; Dearing et al., 2008; Wen et al., 2010). Diatom and ostracod assemblage changes served as eco-indicators for lake water depth changes driven by climatic variations (e.g. Rhodes et al., 1996; Mischke and Wünnemann, 2006; Yan and Wünnemann, 2014). Lake level changes for closed lakes reflected the effective moisture changes responding to different hydrothermal regimes. The descending of lake level normally is a response to dry climate in arid and semi-arid regions of north and northwest China (e.g. Goldsmith et al., 2017; Xu et al., 2017; Yan et al., 2018).

Based on the interpretation and implications of the proxies from the above records, the reported climate inferences were classified into four grades of relative wetness and warmth at *ca.* 4000 cal. yr BP in comparison to the previous stage (e.g. 6.0-4.5 cal. kyr BP) and afterwards (e.g. after *ca.*3.8 cal. kyr BP). Four grades with different codes for wetness were categorised: 1 (drier), 2 (dry), 3 (wet), and 4 (wetter). Similarly, relative warmth was also assigned to 4 codes: 1 (cold), 2 (cool), 3 (moderate), and 4 (warm). Since it is almost impossible to unify different proxies to a consistent wetness or warmth quantitatively, some criteria were adopted for the grade categorizations inspired by Lillios et al. (2016). Grade 1 for wetness (direr) is assigned to the severe dry setting, marked by dramatic decline of lake level or intensified aeolian activities in arid and semi-arid region of north and northwest China (e.g. An et al., 2003; Wen et al., 2010; Yan and Wünnemann, 2014; Scuderi et al., 2019). Grade 2 (dry) is defined as evident declines in the proxies of wetness mentioned above, such as more positive $\delta^{18}O$ values of stalagmite (e.g. Wang et al., 2005; Hu et al., 2008; Zhang et al., 2013) and less precipitation reconstructed from pollen-based estimation (e.g. Xiao et al., 2004; Shen et al., 2005; Liew et al., 2006). Grade 3 (wet) is defined as an increase in proxies of wetness in compassion to the previous stage. Grade 4 (wetter) is described as marketable increases in proxies of wetness. For warmth, grade 1 (cold) is defined as major declines in proxies of warmth especially in north and northwest China where the regions are sensitive to continental air highs and notable decrease in $U_{37}^{K'}$ palaeothermometry. Grade 2 (cool) is interpreted as decreasing warmth in contrast to the previous stage reconstructed from proxies, generally related to the east and south China where relatively warm climates prevail today. Grade 3 (moderate) is defined as slight increase in warmth in comparison to the previous stage. Grade 4 (warm) is portrayed as marked increase in proxies of warmth.

In cases where one site had several records published, all of the records were evaluated individually. We decided to include the ones with multi-proxies (giving priority to pollen and isotope) and a more reliable chronology to ensure a consistent interpretation. Using this, the spatial features of climate and hydrothermal conditions in different climatic zones and topographic regions of China for the time under consideration were illustrated (Fig. 2, Table 1).

2.4. Archaeological data

Information on human occupation such as the pattern of human subsistence, and the temporal and spatial distribution of populaces and artefacts from around 4000 cal. yr BP were extracted from archaeological records and related geo-archaeological studies, referring to publications describing and discussing cultural development and related collapses (e.g., Wu and Wu, 1998; Tian and Tang, 2001; Heritage, Chinese Cultural Atlas Editorial Committee of State Administration of Cultural Heritage, 1997, 2002, 2003, 2006, 2008a, 2008b, 2009, 2011; Wu and Liu, 2004; Fang, 2003; Zhu et al., 2003; An et al., 2005; Chen et al., 2005; Zhang et al., 2005; Tarasov et al., 2006; Hou et al., 2015; Hou et al., 2009; Chen et al., 2011; Liu and Feng, 2012). Cultural collapses in this study are defined as: 1) human migration or exodus indicated by significant loss in the volume and scale of archaeological

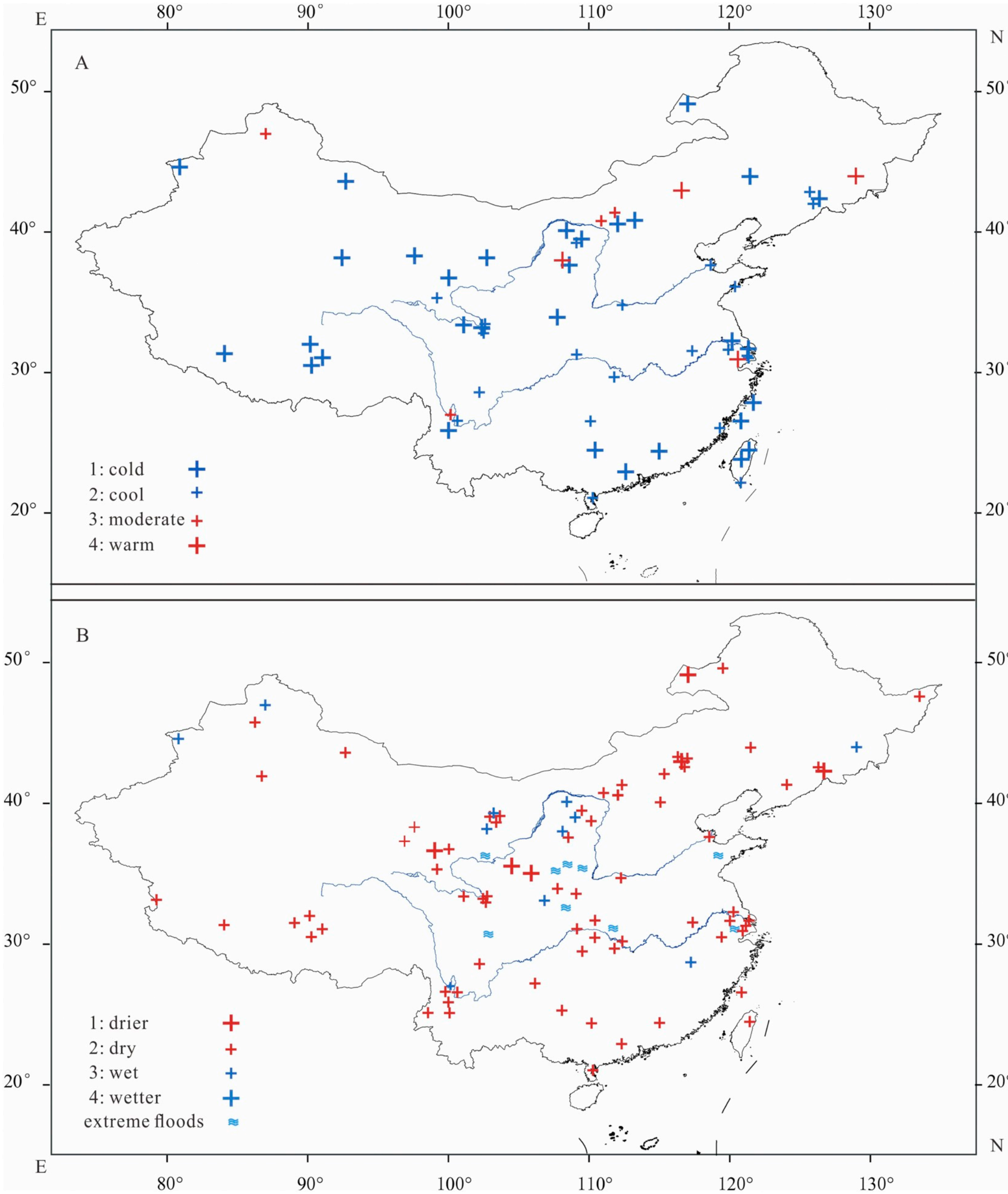

Fig. 2. Summary of climate conditions in terms of warmth and wetness as well as hydrological events documented at selected sites at ca.4000 cal. yr BP. Numbers are referred to sites listed in Tables 1-2.

sites in a given region; 2) a decline in the level of sophistication of artefacts compared to that of preceding cultural phases, and 3) substantial changes and alterations in patterns of subsistence, such as the replacement of agriculture by pastoralism or agro-pastoralism. Those alternations were coupled with selected proxy records from the individual regions that can explain environmental and climate conditions reasonably well for the time interval under consideration.

3. Results

3.1. The spatial distribution of warmth and wetness in China at ca. 4000 cal. yr BP

At a significantly large number of sites (87%, or 53 of 61 sites), a decline in warmth compared to the preceding stage at around 4000 cal. yr BP can be demonstrated by most records, e.g. in those settings which were relatively warm prior to 4500 cal. yr BP (Fig. 2A). Some of the records - in the Tibetan Plateau, the regions of north and northwest China, and monsoonal regions of east China - even exhibit a cold status (Fig. 1, Fig. 2A, Table 1). Relatively warm conditions were reported from few places in northern China and the lower Yangtze River catchment (Fig. 2A, Table 1). For example, pollen and geochemical proxies from lake sediments evidenced a general cold climate in northwest China and the TP such as *ca.* 4.3 cal. kyr BP in Bosten Lake (Mischke and Wünnemann, 2006), *ca.* 4.3-3.8 cal. kyr BP in Balikun Lake (Zhong et al., 2012), *ca.* 4.2-3.7 cal. kyr BP in Manasi Lake (Rhodes et al., 1996), *ca.*4.0-3.7 cal. kyr BP in Nam Co (Mügler et al., 2010), *ca.* 4.0-3.6 cal. kyr BP in Siling Co (Shi et al., 2017), *ca.*4.3-3.4 cal. kyr BP in Bangong Co (Gasse et al., 1996) and *ca.* 4.6-4.0 cal. kyr BP in Cue Lake (Wu et al., 2006). In the northeast of TP, a cold setting with fluctuations at *ca.* 4.5-3.0 cal. kyr BP was also witnessed by multi-proxy data in Kuhai Lake (Wünnemann et al., 2018) and a temperature decline in Qinghai Lake was indicated during *ca.*5.0-3.5 cal. kyr BP by $U_{37}^{K'}$ palaeothermometry (Hou et al., 2015). Along the monsoonal-arid

Table 2
Records of extreme/ catastrophic floods *ca.* 4000 yr BP in China (see Fig. 1 for locations).

Record No.	Location	Proxies	References
a	Yangtze Delta	GS, MS, pollen, minerals	Yu et al., 2000
b	Taihu basin of Yangtze Delta	buried trees and peat	Zhang et al., 2005
c	Jinghe River Gorges	SWD	Huang et al., 2010
d	Qishui River	SWD	Huang et al., 2011, 2012
e	Beiluohe River	SWD	Zhang et al., 2015a
f	Guanting basin	lithology and MS	Ma et al., 2014
g	Guanting basin	flood sediment	Wu et al., 2016
h	Upper Hanjiang River	SWD	Liu et al., 2015c
i	Ankang, upper Hanjiang River	SWD	Zhou et al., 2016
j	Jianghan Plain	flood deposits	Wu et al., 2017
k	Yihe River	flood deposits	Shen et al., 2015
l	Jinsha, Chengdu	buried palaeotrees, Zr/Rb, Ba/Nb, GS	Jia et al., 2017

SWD: slack water deposits; GS: grain-size; MS: magnetic susceptibility;

transition belt, a cold climate prevailed around 4.0 cal. kyr BP except for few sites that showed moderate or warm conditions at sites of Jingbian, south margin of Mu Su desert, Chasuqi, Diaojiao Lake and Haolaihure Lake of central-south inner Mongolia (Wang and Sun, 1997; Xiao et al., 2002; Shi and Song, 2003; Liu et al., 2018). For the monsoonal regions of east and south China, cooling was evident for most of the sites with exceptional ones from Maqiao site of Yangtze delta and Jingpo Lake of northeast China (Yu et al., 2000; Chen et al., 2015). The East China Sea even recorded an extraordinary cold episode at *ca.* 4.4-3.8 cal. kyr BP from $U_{37}^{K'}$ palaeothermometry (Kajita et al., 2018) (Fig. 2A, Table 1).

Reports on changes in humidity or wetness are complex. Most of the records (88%, or 79 of 90 sites) show a transition to dry climate settings in arid regions of northwest China, the TP, the monsoonal and arid transition belt, and monsoonal regions of east and south China around 4000 cal. yr BP (Fig. 1, Fig. 2B, Table 1). Some records even exhibited drier settings. For example, the Hulun Lake of northeastern China and Hala Lake of northeastern TP even underwent dramatic drier conditions at 4.2-3.8 cal. kyr BP and around 4.1 cal. kyr BP inferred by pollen, ostracods result and dramatic declines in lake levels (e.g. Yan and Wünnemann, 2014; Xiao et al., 2018a). The Hunshandake Sandy Lands of northeastern China experienced extreme drying that was exacerbated by lake overflow drainage and sapping with depletion of the groundwater table between 4.2 and 3.8 cal. kyr BP (Scuderi et al., 2019). Exceptions exist at some places in the monsoonal-arid transition belt of north China and in some areas of the Middle to Lower Yangtze River catchment, where relatively wet conditions were indicated (Fig. 2B). For instance, relatively wet conditions occurred at the sites of Sayram Lake and Wulugu Lake of Xinjiang Uygur Autonomous Region (Jiang et al., 2007; Liu et al., 2008), and at some sites of Badain Jaran, Tengger and Mu Su deserts during the period under consideration (Zhang et al., 2000; Chen et al., 2001; Xiao et al., 2002; Chen et al., 2003). One stalagmite record from the Middle to Lower Yangtze River catchment showed humidity increase at around 4.4-3.8 cal. kyr BP although this happened with a drying tendency (Tan et al., 2018). Also, contemporaneous extreme or catastrophic floods are documented in geological records of both the Loess Plateau of the Yellow River basin in north China and the Middle to Lower Yangtze River catchment in south China (e.g. Yu et al., 2000; Zhang et al., 2005; Huang et al., 2010; Liu et al., 2015b; Wu et al., 2016) (Fig. 2B, Table 2).

3.2. Neolithic cultural failures in major topographic regions around 4000 cal. yr BP

According to archaeological findings, the trajectories of Neolithic cultures over a vast region of China were disrupted during the time under consideration. The Laohushan Culture (*ca.* 4500-4100 cal. yr BP) (Fig. 3A), representative of the Neolithic culture of the central Inner Mongolia region, declined in the Lake Daihai basin at its late stage, leaving an approximately 300-year cultural blank before the basin was re-occupied later by the Zhukaigou Culture (*ca.* 3800-3200 cal. yr BP) (Tian and Akiyama, 2001; Xu et al., 2017). In the Liaohe River catchment and north Hebei Plain (Fig. 3B), the number of Neolithic sites decreased significantly during the transition from the early Lower Xiajiadian Culture (*ca.* 4300-4000 cal. yr BP) to the Middle Lower Xiajiadian Culture (*ca.* 4000-3200 cal. yr BP) (Tarasov et al., 2006). In the Gansu-Qinghai region of north-western China (Fig. 3, C1-C2), the Qijia Culture (*ca.* 4300-3900 cal. yr BP) suffered from a dramatic reduction in population and experienced a westward retreat during its late stage. After a brief hiatus of 300 years, the Kayue Culture (*ca.* 3600-2500 cal. yr BP), Xidian Culture (*ca.* 3600-2600 cal. yr BP) and Siwa Culture (*ca.* 3300-2500 cal. yr BP) emerged successively in the region (An et al., 2006; Liu and Feng, 2012). In the Shandong Peninsula of east China (Fig. 4, D1-D2), the Yueshi Culture (*ca.* 4000-3600 cal. yr BP) exhibited a sharp decline in population and shrinking area of occupation in comparison to the previous Longshan Culture, as evidenced by changes in sites (*ca.* 4500-4000 cal. yr BP) (Chen et al., 2011). For the Dongting Lake basin of the Mid-Yangtze River catchment (Fig. 4E), sites of the Shijiahe Culture (*ca.* 4600-4000 cal. yr BP) were distributed densely and even expanded to the hinterland of the lake area during the culture's early and middle stage, but they decreased in site numbers and retreated to the upstream area at its later stage at *ca.* 4000 cal. yr BP (Liu et al., 2012). Along the lower Yangtze River delta (Fig. 4, F1-F2), the Liangzhu Culture (*ca.* 5300-4000 cal. yr BP) had spread to the whole Taihu lake basin during its early and middle stage, but sites were abandoned in large numbers during its late stage after *ca.* 4200 cal. yr BP. The later Maqiao Culture (*ca.* 3800-3200 cal. yr BP) showed a residential concentration behind the high Chenier Ridges of the Lake Taihu basin with limited settlements (Chen et al., 2005; Wu et al., 2014).

4. Discussions

Both social and environmental factors can affect ancient civilization or culture and lead to its collapse or failure, by means of over-exploitation or deterioration of required resources, abrupt climate change, catastrophic events, poor management, tribal invasion or civil war, or an unsustainable treasury or populace. The climate's influence is also believed to be a substantial cause, and climatic events are linked with human conflicts across a range of spatial and temporal scales and across all major regions of the world (Hsiang et al., 2013). In China, strong and significant correlations have been found between climate change, war occurrence, harvest level, population size, and dynastic transitions (Zhang et al., 2006). Thus, the nearly synchronous collapses of Neolithic civilization over a wide territorial span in China around 4000 cal. yr BP could suggest a large-scale driving mechanism related

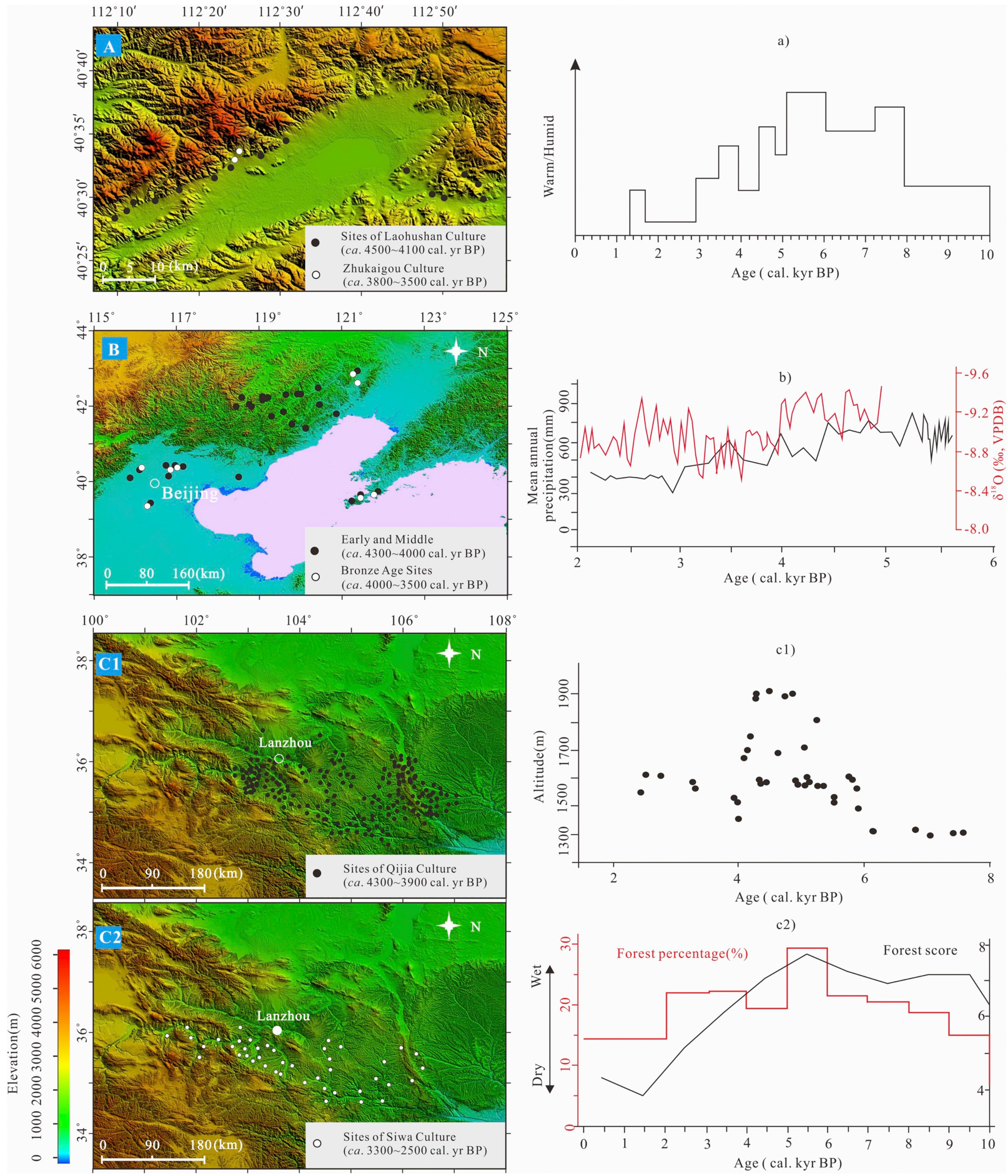

Fig. 3. Climate and Neolithic culture transformations at around 4000 cal. yr BP in Chinese major cultural domain regions. A: the Lake Daihai basin of central-Inner Mongolia (Xu et al., 2017), and (a) the pollen-based warm/humid fluctuations in the basin (Xiao et al., 2004); B: Liaohe River catchment and the north Heibei Plain (modified after Tarasov et al., 2006), and (b) mean annual precipitation reconstruction from pollen record of Taishizhuang peat section(Tarasov et al., 2006) and the $\delta^{18}O$ result from water cave, Benxi, Liaoning Province (Tan and Cai, 2005); C1 and C2: Gansu-Qinghai regions of northwest China and (c1) altitudes of Neolithic sites distributed on the western part of Loess Plateau (modified after An et al., 2006), and (c2) effective moisture levels on the Chinese Loess Plateau indicated by the proportions and biome scores for forest vegetation (Sun et al., 2017a).

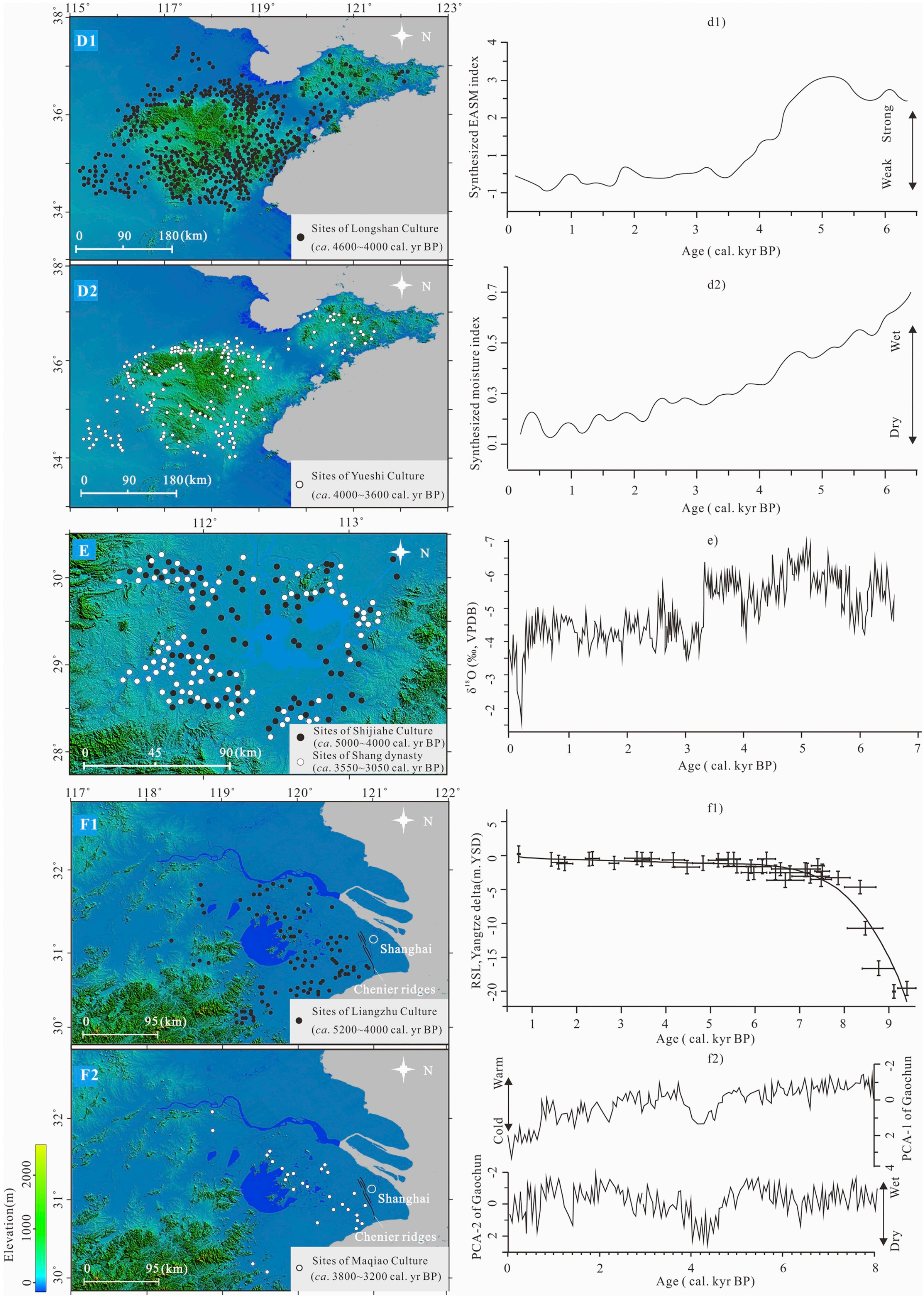

(caption on next page)

Fig. 4. Climate and Neolithic culture transformations at around 4000 cal. yr BP in Chinese major cultural domain regions. D1 and D2: the Shangdong peninsula of eastern China (modified after Chen et al., 2011), and (d1) synthesized East Asia Summer Monsoon index (EASM) of Eastern China (Wang et al., 2010) and (d2) synthesized moisture index from carbonate $\delta^{18}O$ from lake sediments and peat bogs of monsoonal China (Zhao et al., 2009; Zhang et al., 2011).E: Dongting Lake catchment of the middle Yangtze River basin (modified after Liu et al., 2012), and (e) monsoon precipitation changes indicated by the stalagmite $\delta^{18}O$ record of Lianhua cave in Hunan province (Cosford et al., 2008); F1 and F2: the Taihu Lake basin and the Yangtze delta (modified after Chen et al., 2005; Liu et al., 2015c), and (f1) relative sea-level changes (RSL) of the Yangtze delta according to the Yellow Sea datum (YSD) (Zong, 2004), and (f2) warmth and moisture estimations from PCA analysis of a pollen profile at Gaochun, western Taihu lake basin(Yao et al., 2017).

to regional/continental climate change rather than any sole local factor.

4.1. The long trend of the East Asian Summer monsoon

The East Asian monsoon (EAM) winds, driven by seasonal asymmetric heating of land and sea, dominated the climate of China during the Holocene. The inhabitants' livelihoods depended on the monsoon-related precipitation, but they also suffered from droughts and catastrophic flooding disasters related to the high variability of the monsoon climate (An et al., 2015). Since the Middle-Holocene, summer insolation in the Northern Hemisphere has gradually declined with the changes of precession of the Earth's perihelion from the Northern Hemisphere towards the Southern Hemisphere, leading to a southward migration of the Intertropical Convergence Zone (ITCZ) (Wanner et al., 2008; Schneider et al., 2014). As a result, the warm East Asian summer monsoon (EASM) winds that brought moisture northwards, vital to the rain-fed agriculture of inland China, weakened (Wang et al., 2005; Cheng et al., 2012). The pronounced dryness in China around 4000 cal. yr BP could have been a direct response to this long-term decreasing climate trend in both warmth and wetness from the weakened EASM since the Middle-Holocene (Fig. 2).

As the leading driving force, the weakening of the EASM had various impacts on the late Neolithic cultural collapses in climatically and topographically diverse regions of China. In the arid and monsoonal transition regions of northern and north-western China, where agriculture-based civilizations had already flourished for several millennia (Li et al., 2007; Barton et al., 2009; Yang et al., 2012), the weakened EASM around 4000 cal. yr BP would have caused major decreases in precipitation and associated soil moisture along with decreasing warmth, both of which were essential for the rain-fed agriculture. As a result, people were prone to suffer from sustained drought periods and consequential famine. Additionally, steppe vegetation may have become unsuitable for farming but more favourable for pastoralism in these regions under a weaker EASM. Thus, pastoralism or agro-pastoralism seemed to have replaced sedentary agriculture, notably in the arid and monsoonal transition regions. While the deterioration of the climate continued, the migration of Neolithic people to areas with more suitable hydrothermal conditions became the preferred choice for later prehistoric cultures. For instance, in the Daihai Lake basin, archaeological excavations and findings showed that during the Laohushan Culture stage, cave dwelling, pottery making and millet planting prevailed in the lake basin, and well-constructed stone walls around large residential sites hinted a defensive purpose. These things suggested agriculture and sedentary lifestyle rather than pasturing and nomadism were the major characteristics of livelihood in the basin during *ca.* 4500-4100 cal. yr BP (Tian and Akiyama, 2001; Xu et al., 2017). The amicable climate with more monsoonal precipitation prevailed at ~6800-4100 cal. yr BP (Xiao et al., 2004), would attract the settler to move into the basin. While, a climate deterioration with evident drop in temperature and humidity that occurred at ~4100-3800 cal. yr BP hindered the millet growing and forced the human to migrate to south areas where hydrothermal conditions were more suitable. This climate deterioration resulted in a cultural blank for ~300 years in the Daihai Lake basin before it was re-occupied later by the less sophisticated Zhukaigou Culture at *ca.* 3800-3200 cal. yr BP (Tian and Tang, 2001; Xu et al., 2017). In the Liaohe River catchment of south Inner Mongolia region, human exodus and migration to the south areas were also seen occurring with a decreasing warmth and wetness (Tarasov et al., 2006) (Fig. 3 A-B, a-b). In north-eastern China, comparison of late Neolithic (5-4 cal. kyr BP) and early Bronze Age (4-3 cal. kyr BP) archaeological sites revealed a clear decrease in numbers in the desert regions, but a substantial increase in the south regions of middle to lower reaches of Yellow River as a response to climate deterioration (Guo et al., 2018).

In the Gansu-Qinghai region, the changes in patterns of human subsistence were in accord with a transition to dry climate. Millet cultivation of the Qijia Culture was replaced by pastoralism of the Kayue, Xidian and Siwa Cultures after several centuries of cultural discontinuity. Altitude distribution of the unearthed archaeological sites in the western part of the Chinese Loess Plateau exhibited a notable decline around 4000 cal. yr BP, and people migrated southward to the lower latitude areas for better access to water resources (An et al., 2005) (Fig. 3, C1-C2, c1-c2).The weakening EASM and the associated cold-dry climate would have negatively affected the resources necessary for life such as water accessibility and food yields, leading to the cultural migrations or collapses in these regions.

In the Shandong Peninsula of east China, the hydrothermal settings would have been comparatively better than in arid and semi-arid regions due to its proximity to the ocean, the source of moisture. However, the sites of the Yushi Culture still exhibited a remarkable decline in numbers compared to the preceding Longshan Culture on both hilly and lower alluvial plain areas (Fig. 4, D1-D2). The cold-dry climate caused by a weakening EASM may have disrupted the Longshan Culture and forced people to migrate toward the lower areas and river valleys where water access was easily secured (Gao et al., 2007; Chen et al., 2011) (Fig. 4 d1-d2).

4.2. Human conflicts or local environmental changes in monsoonal regions?

In other monsoonal regions of China, like the Dongting Lake area of the middle Yangtze basin and the Taihu lake catchment of the Lower Yangtze, the reason for the collapses in Neolithic culture around *ca.* 4000 cal. yr BP was more complex (Fig. 4E, F1-F2). Some archaeologists have proposed social explanations as major causes. For example, the collapse of the Shijiahe Culture in the Dongting Lake catchment was primarily attributed to warfare between tribes, and the decline of Liangzhu Culture in Taihu Lake area was ascribed to human over-consumption of natural resources and conflicts between tribes (Zhao, 1999; Yuan, 2013). However, such explanations are debatable, as it remains unclear what really caused social conflicts and synchronous cultural transformations at a large regional scale. Instead, it was suggested that the collapse of the Shijiahe Culture was coeval with the decreasing precipitation and a relatively high level of the Dongting Lake induced by extreme floods (Wu and Wu, 1998; Cosford et al., 2008; Hu et al., 2008; Zhu et al., 2014). As rice is the major food source for the people, the expansion of the lake and a rising water table would have impeded local rice farming, forcing the inhabitants to move to the upstream areas of the lake catchment. Along with the recorded cold-dry climate, human subsistence during the late Shjiahe Culture would have made it unsustainable to continue settling in the hinterland of Dongting lake basin (Fig. 4e).

For the Taihu Lake catchment of the Yangtze delta, the expansion of wetland with elevated water level during the late Liangzhu cultural stage at around 4000 cal. yr BP was also reported (Zong et al., 2011; Long et al., 2014; Liu et al., 2015c). Human occupation on the Yangtze delta in the Neolithic time was closely associated with movement of the shore line due to sea level changes (Chen et al., 2005), but only minor fluctuations of sea-level at this period were indicated, suggesting that there were no direct effects of sea-level rise or marine flooding on the collapse of the Liangzhu Culture (Zong et al., 2011; Song et al., 2013). With the stabilization of sea level, delta build-up would have been enhanced by siltation, resulting in poor drainage from the Taihu Lake basin. A freshwater environment would then have covered an area of two to three times of the present basin (Chen et al., 2005; Innes et al., 2014). The elevation of the water table combined with a cold-dry climate likely impeded human habitation and rice farming, leading to the abandonment of most Liangzhu residences around 4000 cal. yr BP (Fig. 4, F1-F2, f1-f2).

4.3. Catastrophic hydrological events?

Catastrophic events were also considered as one of the major causes of the collapses of the Neolithic cultures in the Middle-to-Lower Yellow River and in the Yangtze River basin (e.g. Yu et al., 2000; Li et al., 2014; Shen et al., 2015). In the Loess plateau, at the time under consideration, slackwater deposits overlapping the Neolithic cultural layers at some sites along the river valleys of the middle Yellow River catchment were reported by Huang et al. (2010). In the Guanting basin of the upper Yellow River valley, Qinghai province, Lajia sites were destroyed by a catastrophic flooding around 4.0 cal. kyr BP (Wu et al., 2016). In the Jianghan plain, Dongting Lake, and the Taihu Lake catchments, muddy deposits covered culture layers in some lower altitude locations and the Shajiahe city walls were partially damaged or completely destroyed by floods (Yu et al., 2003; Zhu et al., 2007; Li et al., 2014; Wu et al., 2017). These pieces of evidence have been used by some scholars to connect catastrophic palaeo-floods to the demise of the Neolithic cultures. But disputes remain: 1) Floods may occur more frequently in a wet and rainy climate setting and may have had more adverse effects on the Neolithic cultures in the wet phases prior to 4000 cal. yr BP. However, few pieces of evidence could support such a causal linkage prior to 4000 cal. yr BP. 2) Although floods were common in the topographically lower regions of eastern and southern China during the monsoon seasons, it is unlikely that the widely distributed and flourishing Neolithic cultures could have been destroyed by one or several floods around 4000 cal. yr BP. There are also highlands for people to survive during the interval of floods. 3) A more likely cause was the catastrophic flood events that were evident during this time interval in some cultural sites along the river valleys of the Loess Plateau, in the lower Yellow River plain, and the Middle to lower Yangtze River basin. However, these all occurred within a cold-dry climate setting as shown in Figs. 2, 3 and 4. This indicates that floods might have destroyed some Neolithic sites, but did not necessarily lead to the collapses of the Neolithic cultures across the entirety of China.

4.4. Centennial to interannual climate factors

On interannual scales, the El Niño-Southern Oscillation (ENSO) is a major source of global climate variability (Ropelewski and Halpert, 1987; Whetton and Rutherfurd, 1994). Extreme climate events such as droughts and floods usually resulted from highly variable precipitation in China. They were closely related to anomalies of the EASM, influenced by the activity of ENSO (Jiang et al., 2006). Commonly, warm ENSO phases are associated with low monsoon rainfall in northern China but high rainfall in south China, and vice versa in the cold ENSO phases (Huang and Wu, 1989; Dai and Wigley, 2000). Historical and modern precipitation records also indicate that past catastrophic floods caused by extreme precipitation in the middle-lower Yangtze catchment correlated well with warm ENSO phases (Zhang et al., 2007; Zhu et al., 2017). The reconstructed Holocene history of ENSO variance showed that the modern ENSO regime was established 4500-3000 years ago, and high amplitudes of ENSO have occurred since then (Haug et al., 2001; Stott et al., 2004; Conroy et al., 2008; Carré et al., 2014) (Fig. 5b, c). This high-amplitude of ENSO suggested that northern China was prone to suffer from more floods (or droughts) due to more (or less) rainfalls during the cold (or warm) ENSO phases, while southern China tended to undergo more extreme rainfalls (droughts) during the warm (cold) ENSO phases. Notably, such a high variability of precipitation overlapped with the decreasing trend of warmth and wetness after *ca.* 4500 cal. yr BP.

On the inter-decadal scale, the Pacific decadal oscillation (PDO) has a strong effect on the EASM and rainfall variations over eastern China (Chang et al., 2000; Zhang and Zhou, 2015; Yang et al., 2017). It has been demonstrated that a positive phase of PDO plays a role in the dry conditions in northern China by weakening the EASM and leads to more droughts on the Loess Plateau (Qian and Zhou, 2014; Tan et al., 2014), whereas enhanced rainfall and flooding happened in the middle to lower reaches of the Yangtze River basin (Wu and Mao, 2016). During the negative phase, rainfall concentrates over north China, resulting in higher than normal precipitation and wetter conditions, but less precipitation and more droughts in South China (Zhou and Huang, 2003; Gu et al., 2005). Previous studies suggest that the PDO has an inter-decadal modulation effect on the global climate through modulating the ENSO-related teleconnections (Gershunov and Barnett, 1998; Chan and Zhou, 2005; Yang et al., 2017). The historical variability of the PDO exhibited a shift from a cool phase toward a warm phase between 5.2 and 3.6 cal. kyr BP (Friddell et al., 2003) and positive PDO-like climate variability was progressively enhanced from south to north in the northeast Pacific at *ca.* 4200 cal. yr BP (Barron and Anderson, 2011). Therefore, the interactions of the PDO and ENSO may have amplified EASM precipitation anomalies on both inter-annual and decadal scales, leading to extreme droughts or catastrophic floods in China under a general cold-dry climate.

The variability of EASM was also influenced by both the North Atlantic Oscillation (NAO) and the Atlantic Multi-decadal Oscillation (AMO) through ocean-atmosphere teleconnection (Gupta et al., 2003; Wang et al., 2009; Sun et al., 2012). The strong freshwater input from glacier melting in the north Atlantic at around 4000 cal. yr BP could have slowed down the North Atlantic Deep Water (NADW) and reduced the intensity of Atlantic Meridional Overturning Circulation (AMOC) (Bond et al., 2001; McManus et al., 2004). This caused cooling in the high altitudes of the northern Hemisphere and intensified the airflow of mid-latitude westerlies (MLW) (Wünnemann et al., 2018), inducing a southward shift of the marine intertropical convergence zone and the weakening of the Asian monsoon system (Chiang et al., 2014). Observations and modelling suggested that the southward westerly jet position would have prevented the low-level monsoonal flow from penetrating into the interior of East Asia (Chiang et al., 2015; Herzschuh et al., 2019), resulting in more spring rainfalls in south-central China and a much drier and colder climate in the northern and northwest regions of China. This effect has been reported from several regions of China and elsewhere (An et al., 2012, Yan et al., 2014; Hou et al., 2015; Tan et al., 2018; Wünnemann et al., 2018; Zhang et al., 2018) and thus may have been an important trigger for widely spread cold-dry climate conditions and the high variability of precipitation in China between roughly 5000 and 3000 cal. yr BP. The prolonged droughts and floods are very unfavourable for both dryland farming (wheat and millet) in north China and irrigation farming like rice planting in south China.

These centennial to inter-annual climate variations seem to have modulated the general declining trend of the EASM since the mid-Holocene (Fig. 5, b-i). This period of aridification, also known as the 4.2 ka event, can be considered to be one of the most severe climatic events during the transition of mid to late Holocene. Outside China it also influenced societies from the Nile basin to the Indus Valley (Krom et al., 2002; Demoski et al., 2009; Wünnemann et al., 2010; Dixit et al., 2014; Dutt et al., 2018), the latter known as Harappan Culture. In China this period of weakened monsoon resulted in unstable conditions for human

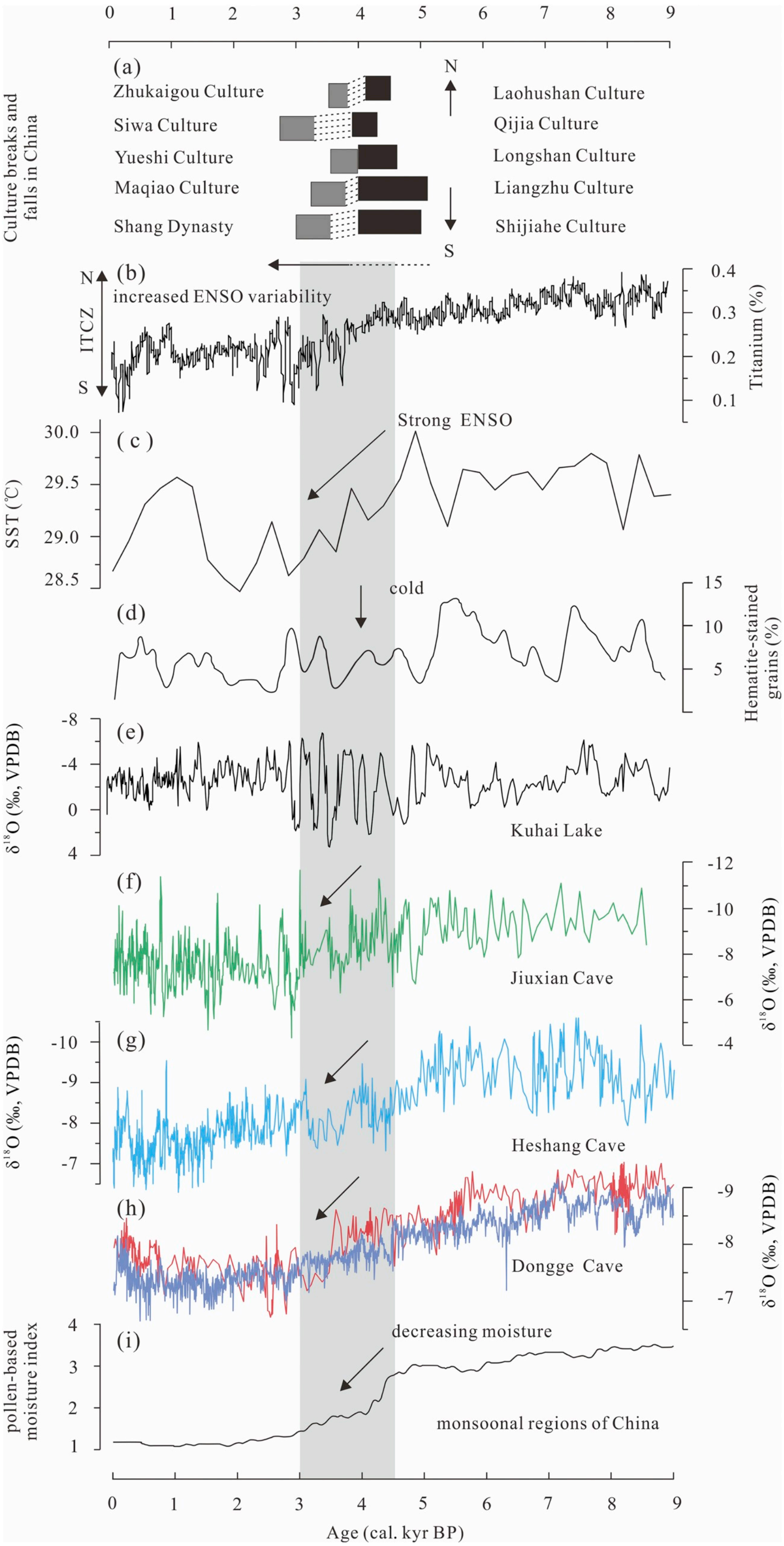

Fig. 5. a) cultural transformations around 4000 *ca.* cal yr BP in the major territory domains of China; b)bulk Ti content of Cariaco Basin sediments from ODP Site 1002, spanning the last 12 kyr (Haug et al., 2001);c) faunal-based SST from MD81 of West Pacific (Stott et al., 2004); d) hematite-stained grains record from stack of MC52-V29191 + MC21-GGc22 of North Atlantic (Bond et al., 2001); e) carbonate oxygen isotope of sediments from lake Kuhai of Tibetan Plateau (Wünnemann et al., 2018);f) Oxygen isotope of stalagmite from Jiuxian Cave in central China (Cai et al., 2010);g) Oxygen isotope of stalagmite from Heshang Cave in central China (Hu et al., 2008); h)Oxygen isotope of stalagmite from Dongge Cave in southwest China (Dykoski et al., 2005; Wang et al., 2005); i) moisture reconstruction based on pollen records in monsoonal regions of China (Zhao et al., 2009). Significant changes around 4000 cal yr BP were revealed by these records.

subsistence, accompanied by the increase of extreme floods and droughts as indicated in the geological records. While the technical advancement and societal complexity were unable to adapt to such large and rapid changes of hydroclimatic conditions, prehistoric civilizations likely collapsed in the major cultural territories of China.

5. Conclusions

The geological records in the climatically and topographically diverse regions of China exhibited a general cold and dry setting around 4000 cal. yr BP, accompanied by extreme droughts and floods in the middle to lower reaches of both the Yellow River and the Yangtze River Basin. This assumption casts some doubt on the previous framework of "drought in the north and flooding in the south of China" at that time. The nearly synchronous collapses of Neolithic cultures around that time interval would suggest a large-scale multiple-source driving mechanism related to the weakening and high variability of the EASM, modulated by global to regional air-sea-land interactions from centennial to inter-annual time scales. They were likely linked with the southward migration of the ICTZ and the westerly jet, the intensity and amplitude of the PDO and ENSO, and changes in the NAO and AMOC. These driving forces would have aggravated the underlying environment in the major Neolithic sedentary territories of China, leading to subsistence difficulties, social conflicts, human migration, and collapses of Neolithic cultures around 4000 cal. yr BP.

Acknowledgements

We wish to thank Dr. D. D. Yan for her useful discussions during the preparation of submission. We also thank the anonymous reviewers and the editor for their constructive suggestions. This study was financially supported by the National Natural Science Foundation of China (Grant Nos. 41671199, 41272194, 41771226 and 41620104004), the National Basic Research Program of China (2015CB953804).

References

An, C.B., Feng, Z.D., Tang, L.Y., 2003. Evidence of a humid mid-Holocene in the western part of Chinese Loess Plateau. Chin. Sci. Bull. 48, 2472–2479.

An, C.B., Tang, L.Y., Barton, L., Chen, F.H., 2005. Climate change and cultural response around 4000 cal yr BP in the western part of Chinese Loess Plateau. Quat. Res. 63, 347–352.

An, C.B., Feng, Z.D., Barton, L., 2006. Dry or humid? Mid-Holocene humidity changes in arid and semi-arid China. Quat. Sci. Rev. 25, 351–361.

An, C.B., Lu, Y., Zhao, J.J., Tao, S.C., Dong, W.M., Li, H., Jin, M., Wang, Z.L., 2012. A high-resolution record of Holocene environmental and climatic changes from Lake Balikun (Xinjiang, China): implications for central Asia. Holocene 22, 43–52.

An, Z.S., Wu, G.X., Li, J.P., Sun, Y.B., Liu, Y.M., Zhou, W.J., Cai, Y.J., Duan, A.M., Li, L., Mao, J.Y., Cheng, H., Shi, Z.G., Tan, L.C., Yan, H., Ao, H., Chang, H., Feng, J., 2015. Global monsoon dynamics and climate change. Annu. Rev. Earth Planet. Sci. 43, 29–77.

Anderson, D.G., Maasch, K.A., Sandweiss, D.H., Mayewski, P.A., 2007. Climate and culture change: exploring Holocene transitions. In: Anderson, D.G., Maasch, K.A., Sandweiss, D.H. (Eds.), Climate Change and Cultural Dynamics. A Global Perspective on Mid-Holocene Transitions. Academic Press, San Diego, pp. 1–23.

Barron, J.A., Anderson, L., 2011. Enhanced Late Holocene ENSO/PDO expression along the margins of the eastern North Pacific. Quat. Int. 235, 3–12.

Barton, L., Newsome, S.D., Chen, F.H., Wang, H., Guilderson, T.P., Bettinger, R.L., 2009. Agricultural origins and the isotopic identity of domestication in northern China. Proc. Natl. Acad. Sci. U. S. A. 106, 5523–5528.

Bond, G., Kromer, B., Beer, J., Muscheler, R., Evans, M.N., Showers, W., Hoffmann, S., Lotti-Bond, R., Hajdas, I., Bonani, G., 2001. Persistent solar influence on North Atlantic climate during the Holocene. Science 294, 2130–2136.

Booth, R.K., Jackson, S.T., Forman, S.L., Kutzbach, J.E., Bettis, E.A., Kreig, J., Wright, D.K., 2005. A severe centennial-scale drought in mid-continental North America 4200 years ago and apparent global linkages. Holocene 15, 321–328.

Cai, Y.J., Tan, L.C., Cheng, H., An, Z.S., Edwards, R.L., Kelly, M.J., Kong, X.G., Wang, X.F., 2010. The variation of summer monsoon precipitation in central China since the last deglaciation. Earth Planet. Sci. Lett. 291, 21–31.

Carré, M., Sachs, J.P., Purca, S., Schauer, A.J., Braconnot, P., Falcón, R.A., Julien, M., Lavallée, D., 2014. Holocene history of ENSO variance and asymmetry in the eastern tropical Pacific. Science 345, 1045–1048.

Chan, J.C.L., Zhou, W., 2005. PDO, ENSO and the early summer monsoon rainfall over south China. Geophys. Res. Lett. 32, L08810. https://doi.org/10.1029/2004GL022015.

Chang, C.P., Zhang, Y.S., Li, T., 2000. Interannual and interdecadal variations of the East Asian summer monsoon and tropical Pacific SSTs. Part I: Roles of the subtropical ridge. J. Climate 13, 4310–4325.

Chen, W., Wang, W.M., 2012. Middle-Late Holocene vegetation history and environment changes revealed by pollen analysis of a core at Qingdao of Shandong Province, East China. Quat. Int. 254, 68–72.

Chen, F.H., Shi, Q., Wang, J.M., 1999. Environmental changes documented by sedimentation of Lake Yiema in arid China since the Late Glaciation. J. Paleolimnol. 22, 159–169.

Chen, F.H., Zhu, Y., Li, J.J., Shi, Q., Jin, L.Y., Wünemann, B., 2001. Abrupt Holocene changes of the Asian monsoon at millennial-and centennial-scales: Evidence from lake sediment document in Minqin Basin, NW China. Chin. Sci. Bull. 46, 1942–1947.

Chen, C.-T.A., Lan, H.-C., Lou, J.-Y., Chen, Y.-C., 2003. The dry Holocene megathermal in inner Mongolia. Palaeogeogr. Palaeoclimatol. Palaeoecol. 193, 181–200.

Chen, Z.Y., Wang, Z.H., Schneiderman, J., Tao, J., Cai, Y.L., 2005. Holocene climate fluctuations in the Yangtze delta of eastern China and the Neolithic response. Holocene 15, 915–924.

Chen, D.D., Peng, S.Z., Zhang, W., Han, J.Q., Ding, M., 2011. The response to Holocene climatic events of Shandong and their impacts on human activity. Prog. Geogr. 30, 846–852 (in Chinese).

Chen, R., Shen, J., Li, C., Zhang, E.L., Sun, W.W., Ji, M., 2015. Mid-to late-Holocene East Asian summer monsoon variability recorded in lacustrine sediments from Jingpo Lake, Northeastern China. Holocene 25, 454–468.

Cheng, H., Sinha, A., Wang, X.F., Cruz, F.W., Edwards, R.L., 2012. The Global Paleomonsoon as seen through speleothem records from Asia and the Americas. Clim. Dyn. 39, 1045–1062.

Chiang, J.C.H., Lee, S.Y., Putnam, A.E., Wang, X.F., 2014. South Pacific Split Jet, ITCZ shifts, and atmospheric North-South linkages during abrupt climate changes of the last glacial period. Earth Planet. Sci. Lett. 406, 233–246.

Chiang, J.C.H., Fung, I.Y., Wu, C.H., Cai, Y.H., Edman, J.P., Liu, Y.W., Day, J.A., Bhattacharya, T., Mondal, Y., Labrousse, C.A., 2015. Role of seasonal transitions and westerly jets in East Asian paleoclimate. Quat. Sci. Rev. 108, 111–129.

Chinese Cultural Atlas Editorial Committee of State Administration of Cultural Heritage, 1997. Chinese Cultural Atlas-Hubei Volume. Hunan Cartongraphic Publishing House, Changsha.

Chinese Cultural Atlas Editorial Committee of State Administration of Cultural Heritage, 2002. Chinese Cultural Atlas-Hubei Volume. Xi'an Cartongraphic Publishing House, Xi'an.

Chinese Cultural Atlas Editorial Committee of State Administration of Cultural Heritage, 2003. Chinese Cultural Atlas-Inner Mongolia Volume. Xi'an Cartongraphic Publishing House, Xi'an.

Chinese Cultural Atlas Editorial Committee of State Administration of Cultural Heritage, 2006. Chinese Cultural Atlas-Qinghai Volume. China Cartographic Publishing House, Beijing.

Chinese Cultural Atlas Editorial Committee of State Administration of Cultural Heritage, 2008a. Chinese Cultral Atlas-Shandong Volume Beijing. China Cartographic Publishing, House.

Chinese Cultural Atlas Editorial Committee of State Administration of Cultural Heritage, 2008b. Chinese Cultrual Atlas-Jiangsu Volume. China Cartographic Publishing House, Beijing.

Chinese Cultural Atlas Editorial Committee of State Administration of Cultural Heritage, 2009. Chinese Cultural Atlas-Zhejiang Volume. Cultural Relics Press, Beijing.

Chinese Cultural Atlas Editorial Committee of State Administration of Cultural Heritage, 2011. Chinese Cultural Atlas-Gansu Volume. Surveying and Maping Press, Beijing.

Clarke, J., Brooks, N., Banning, E.B., Bar-Matthews, M., Campbell, S., Clare, L., Cremaschi, M., di Lernia, S., Drake, N., Gallinaro, M., Manning, S., Nicoll, K., Philip, G., Rosen, S., Schoop, U.D., Tafuri, M.A., Weninger, B., Zerboni, A., 2016. Climatic changes and social transformations in the Near East and North Africa during the 'long' 4th millennium BC: A comparative study of environmental and archaeological evidence. Quat. Sci. Rev. 136, 96–121.

Conroy, J.L., Overpeck, J.T., Cole, J.E., Shanahan, T.M., Steinitz-Kannan, M., 2008. Holocene changes in eastern tropical Pacific climate inferred from a Galápagos lake sediment record. Quat. Sci. Rev. 27, 1166–1180.

Cosford, J., Qing, H.R., Eglington, B., Mattey, D., Yuan, D.X., Zhang, M.L., Cheng, H., 2008. East Asian monsoon variability since the Mid-Holocene recorded in a high-resolution, absolute-dated aragonite speleothem from eastern China. Earth Planet. Sci. Lett. 275, 296–307.

Cullen, H.M., Demenocal, P.B., Hemming, S.R., Hemming, G., Brown, F.H., Guilderson, T.P., Sirocko, F., 2000. Climate change and the collapse of the Akkadian empire: Evidence from the deep sea. Geology 28, 379–382.

Dai, A.G., Wigley, T.M.L., 2000. Global patterns of ENSO-induced precipitation. Geophys. Res. Lett. 27, 1283–1286.

Dearing, J., Jones, R., Shen, J., Yang, X., Boyle, J., Foster, G., Crook, D., Elvin, M., 2008. Using multiple archives to understand past and present climate-human-environment interactions: the lake Erhai catchment, Yunnan Province, China. J. Paleolimnol. 40, 3–31.

deMenocal, P.B., 2001. Cultural responses to climate change during the Late Holocene. Science 292, 667–673.

Demske, D., Tarasov, P.E., Wuennemann, B., Riedel, F., 2009. Late glacial and Holocene vegetation, Indian monsoon and westerly circulation in the Trans-Himalaya recorded in the lacustrine pollen sequence from Tso Kar, Ladakh, NW India. Paleogeogr. Paleoclimatol. Paleoecol. 279, 172–185.

Dixit, Y., Hodell, D.A., Petrie, C.A., 2014. Abrupt weakening of the summer monsoon in northwest India similar to 4100 yr ago. Geology 42, 339–342.

Dong, G.H., Xia, Z.K., Elston, R., Sun, X.W., Chen, F.H., 2009. Response of geochemical records in lacustrine sediments to climate change and human impact during middle Holocene in Mengjin, Henan Province, China. Front. Earth Sci. China 3, 279–285.

Dutt, S., Gupta, A.K., Wunnemann, B., Yan, D.D., 2018. A long arid interlude in the Indian summer monsoon during similar to 4,350 to 3, 450 cal. yr BP contemporaneous to displacement of the Indus valley civilization. Quat. Int. 482, 83–92.

Dykoski, C.A., Edwards, R.L., Cheng, H., Yuan, D.X., Cai, Y.J., Zhang, M.L., Lin, Y.S., Qing, J.M., An, Z.S., Revenaugh, J., 2005. A high-resolution, absolute-dated Holocene and deglacial Asian monsoon record from Dongge Cave, China. Earth Planet. Sci. Lett. 233, 71–86.

Fan, B., Xu, S.Y., Yu, L.Z., Jiang, H., Ran, L.H., 2006. Phytolith in the sediment of the Lake Chaohu since Middle Holocene and its paleoenvironmental implications. J. Lake Sci. 18, 273–279 In Chinese.

Fang, H., 2003. Tentative studies on the decline of Yueshi Culture. J. Literat. Hist. Philos. 3, 139–143.

Feng, Z.D., Wang, W.G., Guo, L.L., Khosbayar, P., Narantsetseg, T., Jull, A.J.T., An, C.B.,

Li, X.Q., Zhang, H.C., Ma, Y.Z., 2005. Lacustrine and eolian records of Holocene climate changes in the Mongolian Plateau: preliminary results. Quat. Int. 136, 25–32.
Friddell, J.E., Thunell, R.C., Guilderson, T.P., Kashgarian, M., 2003. Increased northeast Pacific climatic variability during the warm middle Holocene. Geophys. Res. Lett. 30 (11), 1560. https://doi.org/10.1029/2002GL016834.
Gao, Y.X., 1962. On some problems of Asian monsoon. In: Gao, Y.X. (Ed.), Some Questions about the East Asian Monsoon. Science Press, Beijing, pp. 1–49.
Gao, H.Z., Zhu, C., Xu, W.F., 2007. Environmental change and cultural response around 4200 cal. yr BP in the Yishu River Basin. Shandong. J. Geogr. Sci. 17, 285–292.
Gasse, F., Fontes, J.C., Van Campo, E., Wei, K., 1996. Holocene environmental changes in Bangong Co basin (Western Tibet). Part 4: discussion and conclusions. Palaeogeogr. Palaeoclimatol. Palaeoecol. 120, 79–92.
Gershunov, A., Barnett, T.P., 1998. Interdecadal modulation of ENSO teleconnections. Bull. Am. Meteorol. Soc. 79, 2715–2725.
Goldsmith, Y., Broecker, W.S., Xu, H., Polissar, P.J., deMenocal, P.B., Porat, N., Lan, J.H., Cheng, P., Zhou, W.J., An, Z.S., 2017. Northward extent of East Asian monsoon covaries with intensity on orbital and millennial timescales. Proc. Natl. Acad. Sci. 114, 1817–1821.
Gong, Z.J., Li, S.H., Sun, J.M., Xue, L., 2013. Environmental changes in Hunshandake (Otindag) sandy land revealed by optical dating and multi-proxy study of dune sands. J. Asian Earth Sci. 76, 30–36.
Gu, W., Li, C.Y., Yang, H., 2005. Analysis on interdecadal variation of summer ranifall and its trend in east China. Acta Meteorologica Sinica 63, 728–739.
Guo, L.L., Feng, Z.D., Li, X.Q., Liu, L.Y., Wang, L.X., 2007. Holocene climatic and environmental changes recorded in Baahar Nuur Lake core in the Ordos Plateau, Inner Mongolia of China. Chin. Sci. Bull. 52, 959–966.
Guo, C.X., Luo, F., Ding, X., Luo, Q., Luo, C.X., Cai, Y., Zhao, J., Feng, S., Yang, Z.R., Zhang, J., 2013. Palaeoclimate reconstruction based on pollen records from the Tangke and Riganqiao peat sections in the Zoige Plateau, China. Quat. Int. 286, 19–28.
Guo, Y.Y., Mo, D., Mao, L.J., Guo, W.M., 2016. Environmental changes and human activities around the Youzhougang site in Liyang Plain based on pollen analysis. Geogr. Res. 35, 1041–1050.
Guo, L.C., Xiong, S.F., Ding, Z.L., Jin, G.Y., Wu, J.B., Ye, W., 2018. Role of the mid-Holocene environmental transition in the decline of late Neolithic cultures in the deserts of NE China. Quat. Sci. Rev. 190, 98–113.
Gupta, A.K., Anderson, D.M., Overpeck, J.T., 2003. Abrupt changes in the Asian southwest monsoon during the Holocene and their links to the North Atlantic Ocean. Nature 421, 354–357.
Hao, Q., Liu, H.Y., Yin, Y., Wang, H.Y., Feng, M.M., 2014. Varied responses of forest at its distribution margin to Holocene monsoon development in northern China. Palaeogeogr. Palaeoclimatol. Palaeoecol. 409, 239–248.
Haug, G.H., Hughen, K.A., Sigman, D.M., Peterson, L.C., Röhl, U., 2001. Southward migration of the intertropical convergence zone through the Holocene. Science 293, 1304–1308.
Herzschuh, U., Winter, K., Wünnemann, B., Li, S.J., 2006. A general cooling trend on the central Tibetan Plateau throughout the Holocene recorded by the Lake Zigetang pollen spectra. Quat. Int. 154, 113–121.
Herzschuh, U., Cao, X.Y., Laepple, T., Dallmeyer, A., Telford, R.J., Ni, J., Chen, F., Kong, Z.C., Liu, G.X., Liu, K.B., Liu, X.Q., Stebich, M., Tang, L.Y., Tian, F., Wang, Y.B., Wischnewski, J., Xu, Q.H., Yan, S., Yang, Z.J., Yu, G., Zhang, Y., Zhao, Y., Zheng, Z., 2019. Position and orientation of the westerly jet determined Holocene rainfall patterns in China. Nat. Commun. 10, 8.
Hong, Y.T., Hong, B., Lin, Q.H., Zhu, Y.X., Shibata, Y., Hirota, M., Uchida, M., Leng, X.T., Jiang, H.B., Xu, H., Wang, H., Yi, L., 2003. Correlation between Indian Ocean summer monsoon and North Atlantic climate during the Holocene. Earth Planet. Sci. Lett. 211, 371–380.
Hou, J.Z., Huang, Y.S., Zhao, J.T., Liu, Z.H., Colman, S., An, Z.S., 2015. Large Holocene summer temperature oscillations and impact on the peopling of the northeastern Tibetan Plateau. Geophys. Res. Lett. 43, 1323–1330.
Hou, G.L, Liu, F.G., Liu, C.H, Fang, X.Q., 2009. Prehistorical cultural transition forced by environmental change in Mid-Holocene in Gansu-Qinghai Region. Acta Geograph. Sin. 64, 53–58.
Hsiang, S.M., Burke, M., Miguel, E., 2013. Quantifying the influence of climate on human conflict. Science 341, 1212–1219.
Hu, C.Y., Henderson, G.M., Huang, J.H., Xie, S.C., Sun, Y., Johnson, K.R., 2008. Quantification of Holocene Asian monsoon rainfall from spatially separated cave records. Earth Planet. Sci. Lett. 266, 221–232.
Huang, R.H., Wu, Y.F., 1989. The influence of ENSO on the summer climate change in china and its mechanism. Adv. Atmos. Sci. 6, 21–32.
Huang, C.C., Pang, J.L., Zha, X.C., Zhou, Y.L., Su, H.X., Li, Y.Q., 2010. Extraordinary Floods of 4100− 4000a BP recorded at the Late Neolithic Ruins in the Jinghe River Gorges, Middle Reach of the Yellow River, China. Palaeogeogr. Palaeoclimatol. Palaeoecol. 289, 1–9.
Huang, C.C., Pang, J., Zha, X.C., Su, H.X., Jia, Y.F., 2011. Extraordinary floods related to the climatic event at 4200 a BP on the Qishuihe River, middle reaches of the Yellow River, China. Quat. Sci. Rev. 30, 460–468.
Huang, C.C., Pang, J.L., Zha, X.C., Zhou, Y.L., Su, H.X., Zhang, Y.Z., Wang, H.S., Gu, H.L., 2012. Holocene palaeoflood events recorded by slackwater deposits along the lower Jinghe River valley, middle Yellow River basin, China. J. Quat. Sci. 27, 485–493.
Innes, J.B., Zong, Y.Q., Wang, Z.H., Chen, Z.Y., 2014. Climatic and palaeoecological changes during the mid-to Late Holocene transition in eastern China: high-resolution pollen and non-pollen palynomorph analysis at Pingwang, Yangtze coastal lowlands. Quat. Sci. Rev. 99, 164–175.
Jarvis, D.I., 1993. Pollen evidence of changing Holocene monsoon climate in Sichuan Province, China. Quat. Res. 39, 325–337.
Ji, J.F., Shen, J., Balsam, W., Chen, J., Liu, L.W., Liu, X.Q., 2005. Asian monsoon oscillations in the northeastern Qinghai–Tibet Plateau since the late glacial as interpreted from visible reflectance of Qinghai Lake sediments. Earth Planet. Sci. Lett. 233, 61–70.
Jia, T.J., Ma, C.M., Zhu, C., Guo, T.H., Xu, J.J., Guan, H.C., Zeng, M.X., Huang, M., Zhang, Q., 2017. Depositional evidence of palaeofloods during 4.0-3.6 ka BP at the Jinsha site, Chengdu Plain, China. Quat. Int. 440, 78–89.
Jiang, W.Y., Liu, T.S., 2007. Timing and spatial distribution of mid-Holocene drying over northern China: Response to a southeastward retreat of the East Asian Monsoon. J. Geophys. Res.-Atmos. 112, D24111. https://doi.org/10.1029/2007JD009050.
Jiang, T., Zhang, Q., Zhu, D.M., Wu, Y.J., 2006. Yangtze floods and droughts (China) and teleconnections with ENSO activities (1470-2003). Quat. Int. 144, 29–37.
Jiang, Q.F., Shen, J., Liu, X.Q., Zhang, E., Xiao, X., 2007. A high-resolution climatic change since Holocene inferred from multi-proxy of lake sediment in westerly area of China. Chin. Sci. Bull. 52, 1970–1979.
Jiang, W.Y., Leroy, S.A., Ogle, N., Chu, G.Q., Wang, L., Liu, J.Q., 2008. Natural and anthropogenic forest fires recorded in the Holocene pollen record from a Jinchuan peat bog, northeastern China. Palaeogeogr. Palaeoclimatol. Palaeoecol. 261, 47–57.
Jiang, Q., Ji, J., Shen, J., Matsumoto, R., Tong, G., Qian, P., Ren, X., Yan, D., 2013a. Holocene vegetational and climatic variation in westerly-dominated areas of Central Asia inferred from the Sayram Lake in northern Xinjiang, China. Sci. China Earth Sci. 56 (3), 339–353.
Jiang, X.Y., He, Y.Q., Shen, C.C., Li, Z.Z., Lin, K., 2013b. Replicated stalagmite-inferred centennial- to decadal-scale monsoon precipitation variability in southwest China since the mid Holocene. Holocene 23, 841–849.
Kajita, H., Kawahata, H., Wang, K., Zheng, H.B., Yang, S.Y., Ohkouchi, N., Utsunomiya, M., Zhou, B., Zheng, B., 2018. Extraordinary cold episodes during the mid-Holocene in the Yangtze delta: Interruption of the earliest rice cultivating civilization. Quat. Sci. Rev. 201, 418–428.
Kaniewski, D., Marriner, N., Cheddadi, R., Guiot, J., Van Campo, E., 2018. The 4.2 ka BP event in the Levant. Clim. Past 14, 1529–1542.
Krom, M.D., Stanley, J.D., Cliff, R.A., Woodward, J.C., 2002. Nile River sediment fluctuations over the past 7000 yr and their key role in sapropel development. Geology 30, 71–74.
Kuper, R., Kropelin, S., 2006. Climate-controlled Holocene occupation in the Sahara: motor of Africa's evolution. Science 313, 803–807.
Large, D.J., Spiro, B., Ferrat, M., Shopland, M., Kylander, M., Gallagher, K., Li, X.D., Shen, C.D., Possnert, G., Zhang, G., 2009. The influence of climate, hydrology and permafrost on Holocene peat accumulation at 3500m on the eastern Qinghai–Tibetan Plateau. Quat. Sci. Rev. 28, 3303–3314.
Lee, C.-Y., Liew, P.-M., 2010. Late Quaternary vegetation and climate changes inferred from a pollen record of Dongyuan Lake in southern Taiwan. Palaeogeogr. Palaeoclimatol. Palaeoecol. 287, 58–66.
Li, S.H., Sun, J.M., 2006. Optical dating of Holocene dune sands from the Hulun Buir Desert, northeastern China. Holocene 16, 457–462.
Li, B., Yuan, D.X., Lauritzen, S.E., Qin, J.M., Lin, Y.S., 1998. The Younger Dryas event and holocene climate fluctuations recorded in a stalagmite from the Panlong Cave of Guilin. Acta Geol. Sin. 72, 455–465.
Li, X.Q., Zhou, W.J., An, Z.S., Dodson, J., 2003. The vegetation and monsoon variations at the desert-boess transition belt at Midiwan in northern China for the last 13 ka. Holocene 13, 779–784.
Li, X.Q., Dodson, J., Zhou, X.Y., Zhang, H.B., Masutomoto, R., 2007. Early cultivated wheat and broadening of agriculture in Neolithic China. Holocene 17, 555–560.
Li, B., Zhu, C., Wu, L., Li, F., Sun, W., Wang, X.C., Liu, H., Meng, H.P., Wu, D., 2013. Relationship between environmental change and human activities in the period of the Shijiahe culture, Tanjialing site, Jianghan Plain, China. Quat. Int. 308, 45–52.
Li, F., Zhu, C., Wu, L., Sun, W., Liu, H., Chyi, S.-J., Kung, C.-L., Zhu, G.Y., Wang, X.C., 2014. Environmental humidity changes inferred from multi-indicators in the Jianghan Plain, Central China during the last 12,700 years. Quat. Int. 349, 68–78.
Li, X.Y., Jian, Z.M., Shi, X.F., Liu, S.F., Chen, Z.B., Wu, Y.H., Shi, F.D., 2015. A Holocene record of millennial-scale climate changes in the mud area on the inner shelf of the East China Sea. Quat. Int. 384, 22–27.
Li, N.N., Chambers, F.M., Yang, J.X., Jie, D.M., Liu, L.D., Liu, H.Y., Gao, G.Z., Gao, Z., Li, D.H., Shi, J.C., Feng, Y.Y., Qiao, Z.H., 2017. Records of East Asian monsoon activities in Northeastern China since 15.6 ka, based on grain size analysis of peaty sediments in the Changbai Mountains. Quat. Int. 447, 158–169.
Liew, P., Lee, C., Kuo, C., 2006. Holocene thermal optimal and climate variability of East Asian monsoon inferred from forest reconstruction of a subalpine pollen sequence, Taiwan. Earth Planet. Sci. Lett. 250, 596–605.
Lillios, K.T., Blanco-Gonzalez, A., Drake, B.L., Antonio Lopez-Saez, J., 2016. Mid-late Holocene climate, demography, and cultural dynamics in Iberia: A multi-proxy approach. Quat. Sci. Rev. 135, 138–153.
Lin, R.F., Wei, K.Q., Cheng, Z.Y., Wang, Z.X., Gasse, F., Fontes, J.C., Gibert, E., Tuchoka, P., 1996. A palaeoclimatic study on lacustrine cores from Manas Lake, Xinjiang, western China. Geochimica 25, 63–71 In Chinese.
Liu, F.G., Feng, Z.D., 2012. A dramatic climatic transition at similar to 4000 cal. yr BP and its cultural responses in Chinese cultural domains. The Holocene 22, 1181–1197.
Liu, J.Q., Lu, H.Y., Negendank, J., Mingram, J., Luo, X.G., Wang, W.Y., Chu, G.Q., 2000. Periodicity of Holocene climatic variations in the Huguangyan Maar Lake. Chin. Sci. Bull. 45, 1712–1717.
Liu, X.Q., Dong, H.L., Rech, J.A., Matsumoto, R., Yang, Bo, Wang, Y.B., 2008. Evolution of Chaka Salt Lake in NW China in response to climatic change during the Latest Pleistocene–Holocene. Quat. Sci. Rev. 27, 867–879.
Liu, F.G., Zhang, Y.L., Feng, Z.D., Hou, G.L., Zhou, Q., Zhang, H.F., 2010. The impacts of climate change on the Neolithic cultures of Gansu-Qinghai region during the late Holocene Megathermal. J. Geogr. Sci. 20, 417–430.

Liu, T., Chen, Z.Y., Sun, Q.L., Finlayson, B., 2012. Migration of Neolithic settlements in the Dongting Lake area of the middle Yangtze River basin, China: Lake-level and monsoon climate responses. The Holocene 22, 649–657.
Liu, S.F., Shi, X.F., Liu, Y.G., Wu, Y.H., Yang, G., Wang, X.C., 2013. Holocene paleoclimatic reconstruction based on mud deposits on the inner shelf of the East China Sea. J. Asian Earth Sci. 69, 113–120.
Liu, B., Jin, H.L., Sun, L.Y., Sun, Z., Niu, Q.H., Xie, S.B., Li, G.H., 2014. Holocene moisture change revealed by the Rb/Sr ratio of aeolian deposits in the southeastern Mu Us Desert, China. Aeolian Res. 13, 109–119.
Liu, B., Jin, H.L., Sun, L.Y., Sun, Z., Zhao, S., 2015a. Geochemical evidence for Holocene millennial-scale climatic and environmental changes in the south-eastern Mu Us Desert, northern China. Int. J. Earth Sci. 104, 1889–1900.
Liu, T., Huang, C.C., Pang, J.L., Zha, X.C., Zhou, Y.L., Zhang, Y.Z., Ji, L., 2015b. Late Pleistocene and Holocene palaeoflood events recorded by slackwater deposits in the upper Hanjiang River valley, China. J. Hydrol. 529, 499–510.
Liu, Y., Sun, Q.L., Thomas, I., Zhang, L., Finlayson, B., Zhang, W.G., Chen, J., Chen, Z.Y., 2015c. Middle Holocene coastal environment and the rise of the Liangzhu City complex on the Yangtze delta, China. Quat. Res. 84, 326–334.
Liu, J., Wang, Y., Guan, Y.Y., Dong, J., Li, T.D., 2018. A multi-proxy record of environmental changes during the Holocene from the Haolaihure Paleolake sediments, Inner Mongolia. Quat. Int. 479, 148–159.
Long, H., Lai, Z.P., Wang, N.A., Li, Y., 2010. Holocene climate variations from Zhuyeze terminal lake records in East Asian monsoon margin in arid northern China. Quat. Res. 74, 46–56.
Long, T.W., Qin, J.G., Atahan, P., Mooney, S., Taylor, D., 2014. Rising waters: New geoarchaeological evidence of inundation and early agriculture from former settlement sites on the southern Yangtze Delta, China. Holocene 24, 546–558.
Lu, R.J., Jia, F.F., Gao, S.Y., Shang, Y., Li, J.F., Zhao, C., 2015. Holocene aeolian activity and climatic change in Qinghai Lake basin, northeastern Qinghai–Tibetan Plateau. Palaeogeogr. Palaeoclimatol. Palaeoecol. 430, 1–10.
Ma, C.M., Zhu, C., Zheng, C.G., Wu, C.L., Guan, Y., Zhao, Z.P., Huang, L.Y., Huang, R., 2008. High-resolution geochemistry records of climate changes since late-glacial from Dajiuhu peat in Shennongjia Mountains, Central China. Chin. Sci. Bull. 53, 28–41.
Ma, C.M., Zhu, C., Zheng, C.G., Yin, Q., Zhao, Z.P., 2009. Climate changes in East China since the Late-glacial inferred from high-resolution mountain peat humification records. Sci. China Ser. D Earth Sci. 52, 118–131.
Ma, M.M., Dong, G.H., Chen, F.H., Meng, X.M., Wang, Z.L., Elston, R., Li, G.Q., 2014. Process of paleofloods in Guanting basin, Qinghai Province, China and possible relation to monsoon strength during the mid-Holocene. Quat. Int. 321, 88–96.
Mayewski, P.A., Rohling, E.E., Stager, J.C., Karlen, W., Maasch, K.A., Meeker, L.D., Meyerson, E.A., Gasse, F., van Kreveld, S., Holmgren, K., Lee-Thorp, J., Rosqvist, G., Rack, F., Staubwasser, M., Schneider, R.R., Steig, E.J., 2004. Holocene climate variability. Quat. Res. 62, 243–255.
McManus, J.F., Francois, R., Gherardi, J.M., Keigwin, L.D., Brown-Leger, S., 2004. Collapse and rapid resumption of Atlantic meridional circulation linked to deglacial climate changes. Nature 428, 834–837.
Mischke, S., Wünnemann, B., 2006. The Holocene salinity history of Bosten Lake (Xinjiang, China) inferred from ostracod species assemblages and shell chemistry: possible palaeoclimatic implications. Quat. Int. 154, 100–112.
Mischke, S., Zhang, C.J., 2010. Holocene cold events on the Tibetan Plateau. Glob. Planet. Chang. 72, 155–163.
Mischke, S., Lai, Z.P., Long, H., Tian, F., 2016. Holocene climate and landscape change in the northeastern Tibetan Plateau foreland inferred from the Zhuyeze Lake record. Holocene 26 (4), 643–654.
Mügler, I., Gleixner, G., Günther, F., Mäusbacher, R., Daut, G., Schütt, B., Berking, J., Schwalb, A., Schwark, L., Xu, B., 2010. A multi-proxy approach to reconstruct hydrological changes and Holocene climate development of Nam Co, Central Tibet. J. Paleolimnol. 43, 625–648.
Peng, Y.J., Xiao, J.L., Nakamura, T., Liu, B.L., Inouchi, Y., 2005. Holocene East Asian monsoonal precipitation pattern revealed by grain-size distribution of core sediments of Daihai Lake in Inner Mongolia of north-central China. Earth Planet. Sci. Lett. 233, 467–479.
Qian, C., Zhou, T.J., 2014. Multidecadal variability of North China Aridity and its relationship to PDO during 1900-2010. J. Clim. 27, 1210–1222.
Reimer, P.J., Bard, E., Bayliss, A., Beck, J.W., Blackwell, P.G., Bronk Ramsey, C., Buck, C.E., Cheng, H., Edwards, R.L., Friedrich, M., Grootes, P.M., Guilderson, T.P., Haflidason, H., Hajdas, I., Hatté, C., Heaton, T.J., Hoffmann, D.L., Hogg, A.G., Hughen, K.A., Kaiser, K.F., Kromer, B., Manning, S.W., Niu, M., Reimer, R.W., Richards, D.A., Scott, E.M., Southon, J.R., Staff RA, Turney, C.S.M., van der Plicht, J., 2013. IntCal13 and Marine13 radiocarbon age calibration curves 0–50,000 years cal BP. Radiocarbon 55, 1869–1887.
Rhodes, T.E., Gasse, F., Lin, R.F., Fontes, J.-C., Wei, K.Q., Bertrand, P., Gibert, E., Mélières, F., Tucholka, P., Wang, Z.X., 1996. A late pleistocene-Holocene lacustrine record from Lake Manas, Zunggar (northern Xinjiang, western China). Palaeogeogr. Palaeoclimatol. Palaeoecol. 120, 105–121.
Ropelewski, C.F., Halpert, M.S., 1987. Global and Regional Scale Precipitation Patterns Associated with the El Niño/Southern Oscillation. Mon. Weather Rev. 115, 1606–1626.
Schettler, G., Liu, Q., Mingram, J., Stebich, M., Dulski, P., 2006. East-Asian monsoon variability between 15 000 and 2000 cal. yr BP recorded in varved sediments of Lake Sihailongwan (northeastern China, Long Gang volcanic field). Holocene 16, 1043–1057.
Schneider, T., Bischoff, T., Haug, G.H., 2014. Migrations and dynamics of the intertropical convergence zone. Nature 513, 45–53.
Scuderi, L.A., Yang, X.P., Ascoli, S.E., Li, H.W., 2019. The 4.2 ka BP Event in northeastern China: a geospatial perspective. Clim. Past 15, 367–375.
Selvaraj, K., Chen, C.T.A., Lou, J.Y., 2007. Holocene East Asian monsoon variability: links to solar and tropical Pacific forcing. Geophys. Res. Lett. 34, L01703. https://doi.org/10.1029/2006GL028155.
Shao, X.H., Wang, Y.J., Cheng, H., Kong, X.G., Wu, J.Y., Edwards, R.L., 2006. Long-term trend and abrupt events of the Holocene Asian monsoon inferred from a stalagmite δ10O record from Shennongjia in Central China. Chin. Sci. Bull. 51, 221–228.
Shen, J., Liu, X.Q., Wang, S.M., Matsumoto, R., 2005. Palaeoclimatic changes in the Qinghai Lake area during the last 18,000 years. Quat. Int. 136, 131–140.
Shen, H.Y., Yu, L.P., Zhang, H.M., Zhao, M., Lai, Z.P., 2015. OSL and radiocarbon dating of flood deposits and its paleoclimatic and archaeological implications in the Yihe River Basin, East China. Quat. Geochronol. 30, 398–404.
Shi, P.J., Song, C.Q., 2003. Palynological records of environmental changes in the middle part of Inner Mongolia, China. Chin. Sci. Bull. 48, 1433–1438.
Shi, X.H., Kirby, E., Furlong, K.P., Meng, K., Robinson, R., Lu, H.J., Wang, E., 2017. Rapid and punctuated Late Holocene recession of Siling Co, central Tibet. Quat. Sci. Rev. 172, 15–31.
Song, X.Y., Yao, Y.F., Wortley, A., Paudayal, K., Yang, S.H., Li, C.S., Blackmore, S., 2012. Holocene vegetation and climate history at Haligu on the Jade Dragon snow mountain, Yunnan, SW China. Clim. Chang. 113, 841–866.
Song, B., Li, Z., Saito, Y., Okuno, J.i., Lu, A.Q., Hua, D., Li, J., Li, Y.X., Nakashima, R., 2013. Initiation of the Changjiang (Yangtze) delta and its response to the mid-Holocene sea level change. Palaeogeogr. Palaeoclimatol. Palaeoecol. 388, 81–97.
Staubwasser, M., Sirocko, F., Grootes, P.M., Segl, M., 2003. Climate change at the 4.2 ka BP termination of the Indus valley civilization and Holocene south Asian monsoon variability. Geophys. Res. Lett. 30, 1425. https://doi.org/10.1029/2002GL016822.
Stebich, M., Rehfeld, K., Schlütz, F., Tarasov, P.E., Liu, J.Q., Mingram, J., 2015. Holocene vegetation and climate dynamics of NE China based on the pollen record from Sihailongwan Maar Lake. Quat. Sci. Rev. 124, 275–289.
Stott, L., Cannariato, K., Thunell, R., Haug, G.H., Koutavas, A., Lund, S., 2004. Decline of surface temperature and salinity in the western tropical Pacific Ocean in the Holocene epoch. Nature 431, 56–59.
Sun, A., Feng, Z., 2013. Holocene climatic reconstructions from the fossil pollen record at Qigai Nuur in the southern Mongolian Plateau. The Holocene 23, 1391–1402.
Sun, Y.B., Clemens, S.C., Morrill, C., Lin, X.P., Wang, X.L., An, Z.S., 2012. Influence of Atlantic meridional overturning circulation on the East Asian winter monsoon. Nat. Geosci. 5, 46–49.
Sun, A.Z., Guo, Z.T., Wu, H.B., Li, Q., Yu, Y.Y., Lou, Y.L., Jiang, W.Y., Li, X.Q., 2017a. Reconstruction of the vegetation distribution of different topographic units of the Chinese Loess Plateau during the Holocene. Quat. Sci. Rev. 173, 236–247.
Sun, X.H., Zhao, Y., Li, Q., 2017b. Holocene peatland development and vegetation changes in the Zoige Basin, eastern Tibetan Plateau. Sci. China Earth Sci. 60, 1826–1837.
Tan, M., Cai, B.G., 2005. Preliminary calibration of stalagmite oxygen isotopes from eastern monsoon China with northern Hemisphere temperatures. PAGES News 13, 16–17.
Tan, L.C., An, Z.S., Huh, C.-A., Cai, Y.J., Shen, C.-C., Shiau, L.-J., Yan, L.B., Cheng, H., Edwards, R.L., 2014. Cyclic precipitation variation on the western Loess Plateau of China during the past four centuries. Sci. Rep. 4. https://doi.org/10.1038/srep06381.
Tan, L.C., Cai, Y.J., Cheng, H., Edwards, L.R., Gao, Y.L., Xu, H., Zhang, H.W., An, Z.S., 2018. Centennial- to decadal-scale monsoon precipitation variations in the upper Hanjiang River region, China over the past 6650 years. Earth Planet. Sci. Lett. 482, 580–590.
Tang, L., Wang, X.S., Zhang, S.Q., Chu, G.Q., Chen, Y., Pei, J.L., Sheng, M., Yang, Z.Y., 2015. High-resolution magnetic and palynological records of the last deglaciation and Holocene from Lake Xiarinur in the Hunshandake Sandy Land, Inner Mongolia. Holocene 25, 844–856.
Tao, J., Chen, M.T., Xu, S.Y., 2006. A Holocene environmental record from the southern Yangtze River delta, eastern China. Paleogeogr. Paleoclimatol. Paleoecol. 230, 204–229.
Tao, S.C., An, C.B., Chen, F.H., Tang, L.Y., Wang, Z.L., Lu, Y.B., Li, Z.F., Zheng, T.M., Zhao, J.J., 2010. Pollen-inferred vegetation and environmental changes since 16.7 ka BP at Balikun Lake, Xinjiang. Chin. Sci. Bull. 55, 2449–2457.
Tarasov, P., Jin, G.Y., Wagner, M., 2006. Mid-Holocene environmental and human dynamics in northeastern China reconstructed from pollen and archaeological data. Palaeogeogr. Palaeoclimatol. Palaeoecol. 21, 284–300.
Tarasov, P.E., Demske, D., Leipe, C., Long, T.W., Muller, S., Hoelzmann, P., Wagner, M., 2019. An 8500-year palynological record of vegetation, climate change and human activity in the Bosten Lake region of Northwest China. Palaeogeogr. Palaeoclimatol. Palaeoecol. 516, 166–178.
Tian, G.J., Akiyama, S., 2001. Archaeological excavations at Daihai (II)-A collection of Sino-Japanese Reports and papers on sites in Daihai. Science Press, Beijing, pp. 591 in Chinese.
Tian, G., Tang, X., 2001. A study on the man-environment relation in the Daihai Area of Inner-Mongolia. Collections of Essays On Cniness Historical Geography 16, 4–13.
Turner, B.L., Sabloff, J.A., 2012. Classic Period collapse of the Central Maya Lowlands: Insights about human-environment relationships for sustainability. Proc. Natl. Acad. Sci. U. S. A. 109, 13908–13914.
Wang, B.Y., Sun, X.J., 1997. Primary study on the Holocene environment changes in Chasuqi peat, Inner Mongolia. Chin. Sci. Bull. 42 (5), 514–518 in Chinese.
Wang, R.L, Scarpitta, S., Zhang, S.C, Zheng, M.P., 2002. Later Pleistocene/Holocene climate conditions of Qinghai–Xizhang Plateau (Tibet) based on carbon and oxygen stable isotopes of Zabuye Lake sediments. Earth Planet. Sci. Lett. 203, 461-477.
Wang, Y.J., Cheng, H., Edwards, R.L., He, Y.Q., Kong, X.G., An, Z.S., Wu, J.Y., Kelly, M.J., Dykoski, C.A., Li, X.D., 2005. The Holocene Asian monsoon: links to solar changes

and North Atlantic climate. Science 308, 854–857.
Wang, S.Y., Lu, H.Y., Liu, J.Q., Negendank, J.F., 2007. The early Holocene optimum inferred from a high-resolution pollen record of Huguangyan Maar Lake in southern China. Chin. Sci. Bull. 52, 2829–2836.
Wang, X.Y., Zhang, G.S., Wu, L., Zhang, X.H., Zhang, E.L., Xiao, X.Y., Jiang, Q.F., 2008. Environmental changes during early-middle Holocene from the sediment record of the Chaohu Lake, Anhui Province. Chin. Sci. Bull. 53, 153–160.
Wang, Y.M., Li, S.L., Luo, D.H., 2009. Seasonal response of Asian monsoonal climate to the Atlantic Multidecadal Oscillation. J. Geophys. Res.-Atmos. 114. https://doi.org/10.1029/2008jd010929.
Wang, Y.B., Liu, X.Q., Herzschuh, U., 2010. Asynchronous evolution of the Indian and East Asian Summer Monsoon indicated by Holocene moisture patterns in monsoonal central Asia. Earth Sci. Rev. 103, 135–153.
Wang, L.-C., Behling, H., Chen, Y.-M., Huang, M.-S., Chen, C.-T.A., Lou, J.-Y., Chang, Y.-P., Li, H.-C., 2014. Holocene monsoonal climate changes tracked by multiproxy approach from a lacustrine sediment core of the subalpine Retreat Lake in Taiwan. Quat. Int. 333, 69–76.
Wang, R., Zhang, Y.Z., Wünnemann, B., Biskaborn, B.K., Yin, H., Xia, F., Zhou, L.F., Diekmann, B., 2015. Linkages between Quaternary climate change and sedimentary processes in Hala Lake, northern Tibetan Plateau, China. J. Asian Earth Sci. 107, 140–150.
Wang, H.Y., Song, Y.Q., Cheng, Y., Luo, Y., Zhang, C.N., Gao, Y.S., Qiu, A.A., Deng, L., Liu, H.Y., 2016. Mineral magnetism and other characteristics of sediments from a sub-alpine lake (3080 m a.s.l.) in central east China and their implications on environmental changes for the last 5770 years. Earth Planet. Sci. Lett. 452, 44–59.
Wanner, H., Beer, J., Bütikofer, J., Crowley, T.J., Cubasch, U., Flückiger, J., Goosse, H., Grosjean, M., Joos, F., Kaplan, J.O., 2008. Mid-to Late Holocene climate change: an overview. Quat. Sci. Rev. 27, 1791–1828.
Wanner, H., Solomina, O., Grosjean, M., Ritz, S.P., Jetel, M., 2011. Structure and origin of Holocene cold events. Quat. Sci. Rev. 30, 3109–3123.
Wei, Z.Q., Zhong, W., Shang, S.T., Xue, J.B., Ouyang, J., Zhu, C., Tian, L.X., Chen, Y., Chen, B., 2018. Carbon accumulation in Dahu Swamp in the eastern Nanling Mountains (south China) and its implications for hydroclimatic variability over the past 47000 years. Boreas 47, 469–480.
Weiss, H., Courty, M.A., Wetterstrom, W., Guichard, F., Senior, L., Meadow, R., Curnow, A., 1993. The genesis and collapse of 3rd millennium north mesoptamian civilization. Science 261, 995–1004.
Wen, R.L., Xiao, J.L., Chang, Z.G., Zhai, D.Y., Xu, Q.H., Li, Y.C., Itoh, S., Lomtatidze, Z., 2010. Holocene climate changes in the mid-high-latitude-monsoon margin reflected by the pollen record from Hulun Lake, northeastern Inner Mongolia. Quat. Res. 73, 293–303.
Whetton, P., Rutherfurd, I., 1994. Historical ENSO teleconnections in the Eastern Hemisphere. Clim. Chang. 28, 221–253.
Wu, W.X., Liu, T.S., 2004. Possible role of the "Holocene Event 3" on the collapse of neolithic cultures around the Central Plain of China. Quat. Int. 117, 153–166.
Wu, X.F., Mao, J.Y., 2016. Interdecadal modulation of ENSO-related spring rainfall over South China by the Pacific Decadal Oscillation. Clim. Dyn. 47, 3203–3220.
Wu, X.P., Wu, J.M., 1998. The relationship between the distribution of Neolithic sites and ancient environmental changes in Dongting Lake area. South. Cult. 119, 35–40 (In Chinese).
Wu, Y.H., Lücke, A., Jin, Z.D., Wang, S.M., Schleser, G.H., Battarbee, R.W., Xia, W.L., 2006. Holocene climate development on the central Tibetan Plateau: a sedimentary record from Cuoe Lake. Palaeogeogr. Palaeoclimatol. Palaeoecol. 234, 328–340.
Wu, L., Zhu, C., Zheng, C.G., Li, F., Wang, X.H., Li, L., Sun, W., 2014. Holocene environmental change and its impacts on human settlement in the Shanghai Area, East China. Catena 114, 78–89.
Wu, Q.L., Zhao, Z.J., Liu, L., Granger, D.E., Wang, H., Cohen, D.J., Wu, X.H., Ye, M.L., Bar-Yosef, O., Lu, B., Zhang, J., Zhang, P.Z., Yuan, D.Y., Qi, W.Y., Cai, L.H., Bai, S.B.A., 2016. Outburst flood at 1920 BCE supports historicity of China's Great Flood and the Xia dynasty. Science 353, 579–582.
Wu, L., Zhu, C., Ma, C.M., Li, F., Meng, H.P., Liu, H., Li, L.Y., Wang, X.C., Sun, W., Song, Y.G., 2017. Mid-Holocene palaeoflood events recorded at the Zhongqiao Neolithic cultural site in the Jianghan Plain, middle Yangtze River Valley, China. Quat. Sci. Rev. 173, 145–160.
Wünnemann, B., Demske, D., Tarasov, P., Kotlia, B.S., Reinhardt, C., Bloemendal, J., Diekmann, B., Hartmann, K., Krois, J., Riedel, F., Arya, N., 2010. Hydrological evolution during the last 15 kyr in the Tso Kar lake basin (Ladakh, India), derived from geomorphological, sedimentological and palynological records. Quat. Sci. Rev. 29, 1138–1155.
Wünnemann, B., Yan, D.D., Andersen, N., Riedel, F., Zhang, Y.Z., Sun, Q.L., Hoelzmann, P., 2018. A 14 ka high-resolution delta O-18 lake record reveals a paradigm shift for the process-based reconstruction of hydroclimate on the northern Tibetan Plateau. Quat. Sci. Rev. 200, 65–84.
Xiao, J.L., Nakamura, T., Lu, H.Y., Zhang, G.Y., 2002. Holocene climate changes over the desert/loess transition of north-central China. Earth Planet. Sci. Lett. 197, 11–18.
Xiao, J.L., Xu, Q.H., Nakamura, T., Yang, X.L., Liang, W.D., Inouchi, Y., 2004. Holocene vegetation variation in the Daihai Lake region of north-central China: a direct indication of the Asian monsoon climatic history. Quat. Sci. Rev. 23, 1669–1679.
Xiao, J.L., Si, B., Zhai, D.Y., Itoh, S., Lomtatidze, Z., 2008. Hydrology of Dali Lake in central-eastern Inner Mongolia and Holocene East Asian monsoon variability. J. Paleolimnol. 40, 519–528.
Xiao, X.Y., Haberle, S.G., Shen, J., Yang, X.D., Han, Y., Zhang, E.L., Wang, S.M., 2014. Latest Pleistocene and Holocene vegetation and climate history inferred from an alpine lacustrine record, northwestern Yunnan Province, southwestern China. Quat. Sci. Rev. 86, 35–48.
Xiao, J.L., Zhang, S.R., Fan, J.W., Wen, R.L., Zhai, D.Y., Tian, Z.P., Jiang, D.H., 2018a. The 4.2 ka BP event: multi-proxy records from a closed lake in the northern margin of the East Asian summer monsoon. Clim. Past 14, 1417–1425.
Xiao, X.Y., Haberle, S.G., Li, Y.L., Liu, E.F., Shen, J., Zhang, E.L., Yin, J.J., Wang, S.M., 2018b. Evidence of Holocene climatic change and human impact in northwestern Yunnan Province: High-resolution pollen and charcoal records from Chenghai Lake, southwestern China. Holocene 28, 127–139.
Xie, S.C., Evershed, R.P., Huang, X.Y., Zhu, Z.M., Pancost, R.D., Meyers, P.A., Gong, L.F., Hu, C.Y., Huang, J.H., Zhang, S.H., 2013. Concordant monsoon-driven postglacial hydrological changes in peat and stalagmite records and their impacts on prehistoric cultures in central China. Geology 41, 827–830.
Xu, H., Hong, Y.T., Lin, Q.H., Hong, B., Jiang, H.B., Zhu, Y.X., 2002. Temperature variations in the past 6000 years inferred from δ18O of peat cellulose from Hongyuan, China. Chin. Sci. Bull. 47, 1578–1584.
Xu, L.C., Liu, Y., Sun, Q.L., Chen, J., Cheng, P., Chen, Z.Y., 2017. Climate change and human occupations in the Lake Daihai basin, north-central China over the last 4500 years: A geo-archeological perspective. J. Asian Earth Sci. 138, 367–377.
Yan, D.D., Wünnemann, B., 2014. Late Quaternary water depth changes in Hala Lake, northeastern Tibetan Plateau, derived from ostracod assemblages and sediment properties in multiple sediment records. Quat. Sci. Rev. 95, 95–114.
Yan, D., Wünnemann, B., Zhang, Y.Z., Long, H., Stauch, G., Sun, Q.L., Cao, G.C., 2018. Response of lake-catchment processes to Holocene climate variability: Evidences from the NE Tibetan Plateau. Quat. Sci. Rev. 201, 261–279.
Yang, J.Q., Zhang, W., Cui, Z.J., Yi, C.L., Chen, Y.X., Xu, X.K., 2010. Climate change since 11.5 ka on the Diancang Massif on the southeastern margin of the Tibetan Plateau. Quat. Res. 73, 304–312.
Yang, X.Y., Wan, Z.W., Perry, L., Lu, H.Y., Wang, Q., Zhao, C.H., Li, J., Xie, F., Yu, J.C., Cui, T.X., Wang, T., Li, M.Q., Ge, Q.S., 2012. Early millet use in northern China. Proc. Natl. Acad. Sci. U. S. A. 109, 3726–3730.
Yang, X.P., Scuderi, L.A., Wang, X.L., Scuderi, L.J., Zhang, D.G., Li, H.W., Forman, S., Xu, Q.H., Wang, R.C., Huang, W.W., Yang, S.X., 2015. Groundwater sapping as the cause of irreversible desertification of Hunshandake Sandy Lands, Inner Mongolia, northern China. Proc. Natl. Acad. Sci. U. S. A. 112, 702–706.
Yang, Q., Ma, Z.G., Xu, B.L., 2017. Modulation of monthly precipitation patterns over East China by the Pacific Decadal Oscillation. Clim. Chang. 144, 405–417.
Yao, T.D., Thompson, L.G., 1992. Trends and features of climatic changes in the past 5000 years recorded by the Dunde ice core. Ann. Glaciol. 16, 21–24.
Yao, F.L., Ma, C.M., Zhu, C., Li, J.Y., Chen, G., Tang, L.Y., Huang, M., Jia, T.J., Xu, J.J., 2017. Holocene climate change in the western part of Taihu Lake region, East China. Paleogeogr. Paleoclimatol. Paleoecol. 485, 963–973.
Yasuda, Y., Fujiki, T., Nasu, H., Kato, M., Morita, Y., Mori, Y., Kanehara, M., Toyama, S., Yano, A., Okuno, M., He, J.J., Ishihara, S., Kitagawa, H., Fukusawa, H., Naruse, T., 2004. Environmental archaeology at the Chengtoushan site, Hunan Province, China, and implications for the environmental change and the rise and fall of the Yangtze River civilization. Quat. Int. 123, 149–158.
Yi, S., Saito, Y., Oshima, H., Zhou, Y.Q., Wei, H.L., 2003. Holocene environmental history inferred from pollen assemblages in the Huanghe (Yellow River) delta, China: climatic change and human impact. Quat. Sci. Rev. 22, 609–628.
Yi, S., Saito, Y., Yang, D.-Y., 2006. Palynological evidence for Holocene environmental change in the Changjiang (Yangtze River) delta, China. Palaeogeogr. Palaeoclimatol. Palaeoecol. 241, 103–117.
Yu, S.Y., Zhu, C., Song, J., Qu, W.Z., 2000. Role of climate in the rise and fall of Neolithic cultures on the Yangtze Delta. Boreas 29, 157–165.
Yu, S.Y., Zhu, C., Wang, F.B., 2003. Radiocarbon constraints on the Holocene flood deposits of the Ning-Zhen Mountains, lower Yangtze River area of China. J. Quat. Sci. 18, 521–525.
Yuan, J.P., 2013. City states and Multi-state States in China's early state period Historical Research (in Chinese) 1. pp. 37–53.
Yue, Y., Zheng, Z., Huang, K., Chevalier, M., Chase, B.M., Carré, M., Ledru, M.-P., Cheddadi, R., 2012. A continuous record of vegetation and climate change over the past 50,000 years in the Fujian Province of eastern subtropical China. Palaeogeogr. Palaeoclimatol. Palaeoecol. 365-366, 115–123.
Zhai, D.Y., Xiao, J.L., Zhou, L., Wen, R.L., Chang, Z.G., Wang, X., Jin, X.D., Pang, Q.Q., Itoh, S., 2011. Holocene East Asian monsoon variation inferred from species assemblage and shell chemistry of the ostracodes from Hulun Lake, Inner Mongolia. Quat. Res. 75, 512–522.
Zhang, J., Lin, Z.G., 1992. The Climate of China. Wiley, pp. 376.
Zhang, C.J., Mischke, S., 2009. A Lateglacial and Holocene lake record from the Nianbaoyeze Mountains and inferences of lake, glacier and climate evolution on the eastern Tibetan Plateau. Quat. Sci. Rev. 28, 1970–1983.
Zhang, L.X., Zhou, T.J., 2015. Drought over East Asia: A Review. J. Clim. 28, 3375–3399.
Zhang, H.C., Ma, Y.Z., Wünnemann, B., Pachur, H.-J., 2000. A Holocene climatic record from arid northwestern China. Palaeogeogr. Palaeoclimatol. Palaeoecol. 162, 389–401.
Zhang, Q., Zhu, C., Liu, C.L., Jiang, T., 2005. Environmental change and its impacts on human settlement in the Yangtze Delta, PR China. Catena 60, 267–277.
Zhang, D.D., Jim, C.Y., Lin, G.C.S., He, Y.-Q., Wang, J.J., Lee, H.F., 2006. Climatic change, wars and dynastic cycles in China over the last millennium. Clim. Chang. 76, 459–477.
Zhang, Q., Xu, C.Y., Jiang, T., Wu, Y.J., 2007. Possible influence of ENSO on annual maximum streamflow of the Yangtze River, China. J. Hydrol. 333, 265–274.
Zhang, J.W., Chen, F.H., Holmes, J.A., Li, H., Guo, X.Y., Wang, J.L., Li, S., Lu, Y.B., Zhao, Y., Qiang, M.R., 2011. Holocene monsoon climate documented by oxygen and carbon isotopes from lake sediments and peat bogs in China: a review and synthesis. Quat. Sci. Rev. 30, 1973–1987.
Zhang, H.L., Yu, K.F., Zhao, J.X., Feng, Y.X., Lin, Y.S., Zhou, W., Liu, G.H., 2013. East Asian Summer Monsoon variations in the past 12.5 ka: High-resolution δ18O record

from a precisely dated aragonite stalagmite in central China. J. Asian Earth Sci. 73, 162–175.
Zhang, Y.Z., Huang, C.C., Pang, J.L., Zha, X.C., Zhou, Y.L., Wang, X.Q., 2015a. Holocene palaeoflood events recorded by slackwater deposits along the middle Beiluohe River valley, middle Yellow River basin, China. Boreas 44, 127–138.
Zhang, Z.Q., Zhong, J.J., Lv, X.G., Tong, S.Z., Wang, G.P., 2015b. Climate, vegetation, and human influences on late-Holocene fire regimes in the Sanjiang plain, northeastern China. Palaeogeogr. Palaeoclimatol. Palaeoecol. 438, 1–8.
Zhang, E.L., Zhao, C., Xue, B., Liu, Z.H., Yu, Z.C., Chen, R., Shen, J., 2017. Millennial-scale hydroclimate variations in southwest China linked to tropical Indian Ocean since the Last Glacial Maximum. Geology 45, 435–438.
Zhang, H.W., Cheng, H., Cai, Y.J., Spotl, C., Kathayat, G., Sinha, A., Edwards, R.L., Tan, L.C., 2018. Hydroclimatic variations in southeastern China during the 4.2 ka event reflected by stalagmite records. Clim. Past 14, 1805–1817.
Zhao, H., 1999. Some characteristics of the Liangzhu culture. Zhejiang Institute of Archaeology, Liangzhu Wenhua Yanjiu, pp. 104–119 (in Chinese).
Zhao, Y., Yu, Z.C., Chen, F.H., Zhang, J.W., Yang, B., 2009. Vegetation response to Holocene climate change in monsoon-influenced region of China. Earth Sci. Rev. 97, 242–256.
Zhao, C., Yu, Z.C., Zhao, Y., Ito, E., Kodama, K.P., Chen, F.H., 2010. Holocene millennial-scale climate variations documented by multiple lake-level proxies in sediment cores from Hurleg Lake, Northwest China. J. Paleolimnol. 44, 995–1008.
Zhao, W., Zhao, Y., Qin, F., 2017. Holocene fire, vegetation, and climate dynamics inferred from charcoal and pollen record in the eastern Tibetan Plateau. J. Asian Earth Sci. 147, 9–16.
Zhao, S., Xia, D.S., Jin, H.L., Jia, J., Liu, B., 2018. A multi-proxy late Holocene climate record from aeolian deposits of the Horqin sandy land, northeast China and its societal implications. Aeolian Res. 35, 29–38.
Zheng, H.B., Zhou, Y.S., Yang, Q., Hu, Z.J., Ling, G.J., Zhang, J.Z., Gu, C.G., Wang, Y.Y., Cao, Y.T., Huang, X.R., Cheng, Y., Zhang, X.Y., Wu, W.X., 2018. Spatial and temporal distribution of Neolithic sites in coastal China: Sea level changes, geomorphic evolution and human adaption. Science China-Earth Sciences 61, 123–133.
Zhong, W., Pen, Z.H., Xue, J.B., Ouyang, J., Tang, X.H., Cao, J.Y., 2012. Geochemistry of sediments from Barkol Lake in the westerly influenced northeast Xinjiang: Implications for catchment weathering intensity during the Holocene. J. Asian Earth Sci. 50, 7–13.
Zhong, W., Xue, J.B., Ouyang, J., Tang, X.H., Yin, H.L., Liao, C.Y., Long, K., 2014. Late Holocene monsoon climate as evidenced by proxy records from a lacustrine sediment sequence in western Guangdong, South China. J. Asian Earth Sci. 80, 56–62.
Zhong, W., Cao, J.Y., Xue, J.B., Ouyang, J., 2015. A 15,400-year record of climate variation from a subalpine lacustrine sedimentary sequence in the western Nanling Mountains in South China. Quat. Res. 84, 246–254.
Zhou, L.T., Huang, R.H., 2003. Research on the Characteristics of Interdecadal Variability of Summer Climate in China and Its Possible Cause. Clim. Environ. Res. 8, 274–290.
Zhou, W.J., Yu, X.F., Jull, A.T., Burr, G., Xiao, J.Y., Lu, X.F., Xian, F., 2004. High-resolution evidence from southern China of an early Holocene optimum and a mid-Holocene dry event during the past 18,000 years. Quat. Res. 62, 39–48.
Zhou, W.J., Xie, S.C., Meyers, P.A., Zheng, Y.H., 2005. Reconstruction of late glacial and Holocene climate evolution in southern China from geolipids and pollen in the Dingnan peat sequence. Org. Geochem. 36, 1272–1284.
Zhou, L., Huang, C.C., Zhou, Y.L., Pang, J.L., Zha, X.C., Xu, J., Zhang, Y.Z., Guo, Y.Q., 2016. Late Pleistocene and Holocene extreme hydrological event records from slackwater flood deposits of the Ankang east reach in the upper Hanjiang River valley, China. Boreas 45, 673–687.
Zhu, C., Zhang, Q., Zhang, Y., Zhang, Z.H., Shen, M.J., 2003. Relationship Between Human and Nature in the North Part of the Yangtze Delta since the Holocene. Sci. Geogr. Sin. 23, 705–712.
Zhu, C., Zhong, Y.S., Zheng, C.G., Ma, C.M., Li, L., 2007. Relationship of Archaeological Sites Distribution and Environment from the Paleolithic Age to the Warring States Time in Hubei Province. Acta Geograph. Sin. 62, 227–242.
Zhu, C., Chen, X., Zhang, G.S., Ma, C.M., Zhu, Q., Li, Z.X., Xu, W.F., 2008a. Spore-pollen-climate factor transfer function and paleoenvironment reconstruction in Dajiuhu, Shennongjia, Central China. Chin. Sci. Bull. 53, 42–49.
Zhu, L.P., Wu, Y.H., Wang, J.B., Lin, X., Ju, J.T., Xie, M.P., Li, M.H., Mausbacher, R., Schwalb, A., Daut, G., 2008b. Environmental changes since 8.4 ka reflected in the lacustrine core sediments from Nam Co, central Tibetan Plateau, China. Holocene 18, 831–839.
Zhu, C., Ma, C.M., Yu, S.Y., Tang, L.Y., Zhang, W.Q., Lu, X.F., 2010. A detailed pollen record of vegetation and climate changes in Central China during the past 16,000 years. Boreas 39, 9–76.
Zhu, C., Wu, L., Li, L., Zheng, C.G., Li, Z.X., Ma, C.M., Tan, Y., Zhao, Q.H., Wang, K.H., Lin, L.G., Jiang, Z.H., Ding, J.L., Meng, H.P., 2014. Research progress on Holocene environmental archaeology in the Yangtze River Valley, China. Acta Geograph. Sin. 69, 1268–1283.
Zhu, Z.M., Feinberg, J.M., Xie, S.C., Bourne, M.D., Huang, C.J., Hu, C.Y., Cheng, H., 2017. Holocene ENSO-related cyclic storms recorded by magnetic minerals in speleothems of central China. Proc. Natl. Acad. Sci. U. S. A. 114, 852–857.
Zong, Y.Q., 2004. Mid-holocene sea-level highstand along the southeast coast of China. Quat. Int. 117, 55–67.
Zong, Y., Innes, J.B., Wang, Z.H., Chen, Z.Y., 2011. Mid-Holocene coastal hydrology and salinity changes in the east Taihu area of the lower Yangtze wetlands, China. Quat. Res. 76, 69–82.